sustainability

Article

Multi-Criteria Energy Management with Preference Induced Load Scheduling Using Grey Wolf Optimizer

Sara Ayub [1,2,*], Shahrin Md Ayob [1,*], Chee Wei Tan [1], Saad M. Arif [3], Muhammad Taimoor [4], Lubna Aziz [1,2], Abba Lawan Bukar [1,5], Qasem Al-Tashi [6,7] and Razman Ayop [1]

1 Division of Electrical Power Engineering, School of Electrical Engineering, Faculty of Engineering, Universiti Teknologi Malaysia, UTM, Skudai 81310, Johor, Malaysia
2 Department of Electrical Engineering, Faculty of Information and Communication Technology, BUITEMS, Quetta 87300, Pakistan
3 Department of Electrical Engineering, Aligarh Muslim University, Aligarh 202002, India
4 Faculty of Electrical and Computer Engineering, University of Kassel, 34132 Kassel, Germany
5 Department of Electrical and Electronic Engineering, Faculty of Engineering, University of Maiduguri, Borno State, P.O. Box 1069, Maiduguri 600004, Nigeria
6 Department of Imaging Physics, The University of Texas MD Anderson Cancer Center, Houston, TX 78712, USA
7 Faculty of Administrative and Computer Sciences, University of Albaydha, Albaydha CV46+6X, Yemen
* Correspondence: ayub.sara@graduate.utm.my (S.A.); shahrin@fke.utm.my (S.M.A.)

Abstract: Minimizing energy costs while maintaining consumer satisfaction is a very challenging task in a smart home. The contradictory nature of these two objective functions (cost of energy and satisfaction level) requires a multi-objective problem formulation that can offer several trade-off solutions to the consumer. Previous works have individually considered the cost and satisfaction, but there is a lack of research that considers both these objectives simultaneously. Our work proposes an optimum home appliance scheduling method to obtain an optimum satisfaction level with a minimum cost of energy. To achieve this goal, first, an energy management system (EMS) is developed using a rule-based algorithm to reduce the cost of energy by efficient utilization of renewable energy resources and an energy storage system. The second part involves the development of an optimization algorithm for optimal appliance scheduling based on consumer satisfaction level, involving their time and device-based preferences. For that purpose, a multi-objective grey wolf accretive satisfaction algorithm (MGWASA) is developed, with the aim to provide trade-off solutions for optimal load patterns based on cost per unit satisfaction index (Cs_index) and percentage satisfaction (%S). The MGWASA is evaluated for a grid-connected smart home model with EMS. To ensure the accuracy of the numerical simulations, actual climatological data and consumer preferences are considered. The Cs_index is derived for six different cases by simulating (a) optimal load, (b) ideal load, and (c) base (random) load, with and without EMS. The results of MGWASA are benchmarked against other state-of-the-art optimization algorithms, namely, binary non-dominated sorting genetic algorithm-2 (NSGAII), multi-objective binary particle swarm optimization algorithm (MOBPSO), Multi-objective artificial bee colony (MOABC), and multi-objective evolutionary algorithm (MOEA). With the proposed appliance scheduling technique, a % reduction in annual energy cost is achieved. MGWASA yields Cs_index at 0.049$ with %S of 97%, in comparison to NSGAII, MOBPSO, MOABC, and MOEA, which yield %S of 95%, 90%, 92%, and 94% at 0.052$, 0.048$, 0.0485$, and 0.050$, respectively. Moreover, various related aspects, including energy balance, PV utilization, energy cost, net present cost, and cash payback period, are also analyzed. Lastly, sensitivity analysis is carried out to demonstrate the impact of any future uncertainties on the system inputs.

Keywords: energy demand management; home energy management system; grey wolf optimizer; residential load scheduling; alternative energy sources

check for updates

Citation: Ayub, S.; Ayob, S.M.; Tan, C.W.; Arif, S.M.; Taimoor, M.; Aziz, L.; Bukar, A.L.; Al-Tashi, Q.; Ayop, R. Multi-Criteria Energy Management with Preference Induced Load Scheduling Using Grey Wolf Optimizer. *Sustainability* **2023**, *15*, 957. https://doi.org/10.3390/su15020957

Academic Editor: Ramchandra Pode

Received: 2 November 2022
Revised: 8 December 2022
Accepted: 13 December 2022
Published: 4 January 2023

1. Introduction

High residential energy demand has significantly increased energy costs globally. Climate change and pandemics have accelerated global residential energy consumption. In the United States, the residential energy demand has increased many folds, while in the European Union, residential power consumption increased to 26.3% in 2019 [1]. According to the energy information administration, in the last ten years, the rate of residential electricity in the U.S. has risen by 15% [2,3]. Moreover, this trend will likely continue as the estimated 80% additional increase in residential buildings by 2050.

Furthermore, combined with rising fuel prices like coal, natural gases are only likely to increase the electricity rate. However, uncertainty in producing power from renewable energy resources RER caused by the intermittent nature of the RER will lead the utility to face additional operational challenges. The residential sector is one of the most energy-intensive segments and offers considerable scope to implement various power optimization methods and technologies.

Over the years, primary energy sector research has focused on various innovative techniques to address the rising demand for a stable energy system. With the modern smart grid, benefits such as energy usage reduction, cost reduction, and increased overall grid efficiency can be reaped. Managing the residential load demand by effectively scheduling the residential devices is crucial to achieving these benefits. Energy management can be broadly classified into supply-side management (SSM) and demand-side management (DSM). Widespread adoption of DSM by consumers for their home energy management has been reported due to associated economic benefits [4,5]. The concept of demand side management includes all the activities which aim at modifying the consumption load curves focusing on increasing customer benefit and improving system reliability subject to the uncertainties of consumption profile. Several previous research works have emphasized the development of an improved DSM.

Employing renewable energy resources (RERs) for residential energy offers several personal and public benefits. On a personal level, using RERs provides urban consumers with a cost-effective green solution to reduce their dependence on the utility grid and remote energy sources. RERs have little to no carbon emissions compared to fossil fuels, resulting in reduced environmental impact, which helps mitigate global warming. Smart Home Energy Management Systems (SHEMS) integrates RERs and energy storage systems (ESS), improving sustainability, efficiency, energy conservation, and reducing energy costs while coping with ever-increasing energy demand. The most preferred model for smart homes globally comprises a combination of photovoltaic (PV) and ESS to meet the dynamic energy demand. However, climatological conditions, especially solar irradiance, significantly impact energy generation by PV modules [6].

During the COVID-19 pandemic, an increasing number of people have opted for the home office, and some countries even declared work from home a legal right of the people. Spending more time at home has made residential consumers more conscious regarding their quality of life, thus increasing the significance of the consumer satisfaction aspect of energy consumption. The waiting time is considered one of the key evaluation criteria for consumer satisfaction. Therefore many scheduling algorithms aim to reduce the waiting time to achieve a higher consumer satisfaction level [7]. Previous research mostly focused on reducing energy costs but gave trivial satisfaction to the consumers. An adequate consumer satisfaction indicator is necessary to make consumers choose the most cost-optimal load scheduling. Thus, a more holistic load management approach involving consumer satisfaction and energy cost reduction is needed. Few previous works have emphasized the relationship between consumer satisfaction and managing comfort conditions [8–10]. Manzoor et al. elaborated on the relationship between the factors like energy usage, cost, and the level of consumer discomfort. They designed a teacher learning and genetic algorithm-based hybrid optimization algorithm without considering the possibility of renewable energy [11]. The consumer discomfort is aggravated when either the operation time of devices is delayed or the consumer's power demand for power-flexible

devices is compressed. A multi-objective model was proposed by considering factors like consumer satisfaction and the economy, and its effectiveness was demonstrated by numerical simulations [12]. However, the study did not consider the integration of renewable energy. In [13], consumer satisfaction and usage rate of renewable power were considered to develop an optimization algorithm to curtail the daily electricity bill. However, this work considered an off-grid scenario where the system was entirely dependent on renewables, and the utility grid was not considered. Whereas, in [14,15] author uses the state flow method to resolve the problem of load shedding while the author does not consider consumer satisfaction. An algorithm for demand satisfaction was developed to achieve maximum consumer comfort at a minimum price for various budget scenarios [16]. The concept of a two-tier consumer satisfaction [17], i.e., time and device-based satisfactions, was utilized in [18] for optimization by a single objective competitive grey wolf algorithm design to enhance the consumer satisfaction level under a pre-defined budget. The results suggested that higher consumer satisfaction can be achieved with an increasing budget. However, the system is less reliable as it is only dependent on the grid. Furthermore, the comprehensive state of the art is listed in Table 1. ✔ and ✕ sign shows that the reference considered that attribute in the research or not respectively.

Considering the relevant state-of-the-art, the author has found the following research gaps:

- The problem of optimal home appliance scheduling objective considered either reducing the cost or comfort level of the consumer. A pre-defined limited budget leaves the consumer with limited scheduling options; thus, trade-off solutions are needed between the percentage satisfaction and cost per unit satisfaction index.
- In general, the proposed strategies lack the flexibility to adapt to diverse situations and systems. In that context, energy export to the grid, as well as demand response, becomes pertinent features, which are challenging to manage using state-of-the-art strategies because they usually do not consider demand response and prosumer scenarios.
- To the best of the author's knowledge, most of the relevant works have only provided a comparison of results acquired from various demand response incentive programs without considering the effect of RER-based EMS on demand response programs. Furthermore, the current strategies lack the versatility to conduct such comparisons conveniently.

This work develops a novel approach for the comprehensive design of intelligent appliance scheduling with the RER-ESS system at the smart home level, intending to address the aforementioned challenges. The presented strategy is premised on home appliance scheduling, which is raised as a multi-objective problem and solved analytically by developing a novel multi-objective binary grey wolf accretive satisfaction algorithm (MGWASA), providing trade-off solutions between an optimal set of cost with best satisfaction level. Demand response programs are considered by including the time and device preferences of the consumer, along with the different TOU tariffs for all seasons. Unlike previous approaches, the stability of the system is modeled using scenarios, which are based upon actual data and included in the optimization problem. The main contribution of this work and salient features of the proposed methodology includes the following:

(a) Proposes modified consumer satisfaction objectives where the importance of device and operational time is incorporated through time and device preference tables. Novel MGWASA that integrates consumer preferences with RERs in a smart home environment provides trade-off solutions between cost and user satisfaction.
(b) Different scenarios generated through the approach are analyzed to effectively utilize the RERs for improved reliability. For the aforementioned purpose, a rule-based EMS for a smart home, which integrates RERs with the intelligent scheduling of appliances, is also proposed.
(c) To validate the improved efficacy of the proposed MGWASA for versatility and universal applicability, a comparative analysis with the binary non-dominated sorting genetic algorithm-2 (NSGAII), multi-objective binary particle swarm optimization algorithm (MOBPSO), Multi-objective artificial bee colony (MOABC), and multi-objective evolutionary algorithm (MOEA), is also provided.

Table 1. State of the art related to DSM.

S.No	Model	Algorithms (Techniques)	Cost Function				Integration			Limitations		
			Electricity Cost	PAR	UC or Consumer Satisfaction	Single Objective	Multi-Objective	ESS	RER	Scheduling Home Appliances	Selling Capability	Utilizing Main Grid	Supporting Selling Operation
1	RTP model [19]	PSO, BPSO	✔	✔	×	✔	×	✔	✔	✔	✔	✔	✔
2 faCheck	Time-varying prices Model [20]	Stochastic optimization approach	✔	×	×	✔	×	✔	✔	✔	✔	✔	
3	Price-based model [21]	MILP	✔	×	✔	×	✔	✔	✔	✔	✔	✔	✔
4	Price-based Model [22]	MILP	✔	✔	✔	×	✔	×	×	✔	×	✔	×
5	TOU tariff Model [23]	Preference-based load scheduling	✔	✔	×	✔	×	✔	✔	✔	×	✔	×
6	Incentive based model [24]	Data Analytic approach	✔	✔	✔	✔	×	×	×	✔	×	✔	×
7	Incentive based model [25]	BILP optimization	✔	×	✔	✔	×	×	×	✔	×	✔	×
8	Real-time electricity pricing [26]	Smart energy Coordination scheme	✔	✔	×	×	✔	✔	✔	✔	✔	✔	✔
9	Price-based Model	MOGWO	✔	✔	✔	×	✔	×	×	✔	×	✔	×
10	Proposed Approach (TOU)	MGWASA	✔	×	✔	×	✔	✔	✔	✔	✔	✔	✔

The rest of the article is structured as follows: Section 2 presents the architecture of the proposed test case system. Section 3 describes the modeling and parameters of different smart home units, including PV, ESS, preference, and satisfaction. Section 4 illustrates the climatological conditions and energy demand of the study location. Section 5 presents the proposed EMS and its modes of operation. Section 6 introduces the proposed MGWASA-based intelligent EMS and formulates the problem of the case study. Section 7 presents, discusses, and analyzes the simulation results. The conclusion drawn from the work and outlook is provided in Section 8.

2. The Architecture of the Proposed Test Case System

The decision to switch on or off a device is based on factors like supplied energy from the utility grid and PV, the status of the batteries, and consumer preferences. In this work, the pricing scheme considers a time of use (TOU) pricing policy used in Quetta, Pakistan. An overview of SHEMS architecture is shown in Figure 1 to provide a holistic picture. SHEMS consists of a central controller with intelligent EMS and a scheduler. Central controller with EMS takes other parameters like available PV energy and level of stored energy in the ESS and regulates them according to the load demand of the consumer. On the other hand, the scheduler takes the estimated values of PV energy and *SOC* of the ESS and provides day a head optimal scheduling pattern of appliances. The load consists of the appliances divided into a section of the small home, as shown in Figure 1. Appliances are scheduled according to the algorithms executed via the scheduler, thus making it the most vital module of the SHEMS. The scheduler utilizes a user interface to acquire the day-ahead energy usage demand for individual time slots from the smart home consumer. Moreover, the appliance manager uses this schedule to control the switching activities of the appliances via the home area network (HAN). The HAN is an in-home private network that interconnects appliances with the appliance manager using wireless or/and wired technologies.

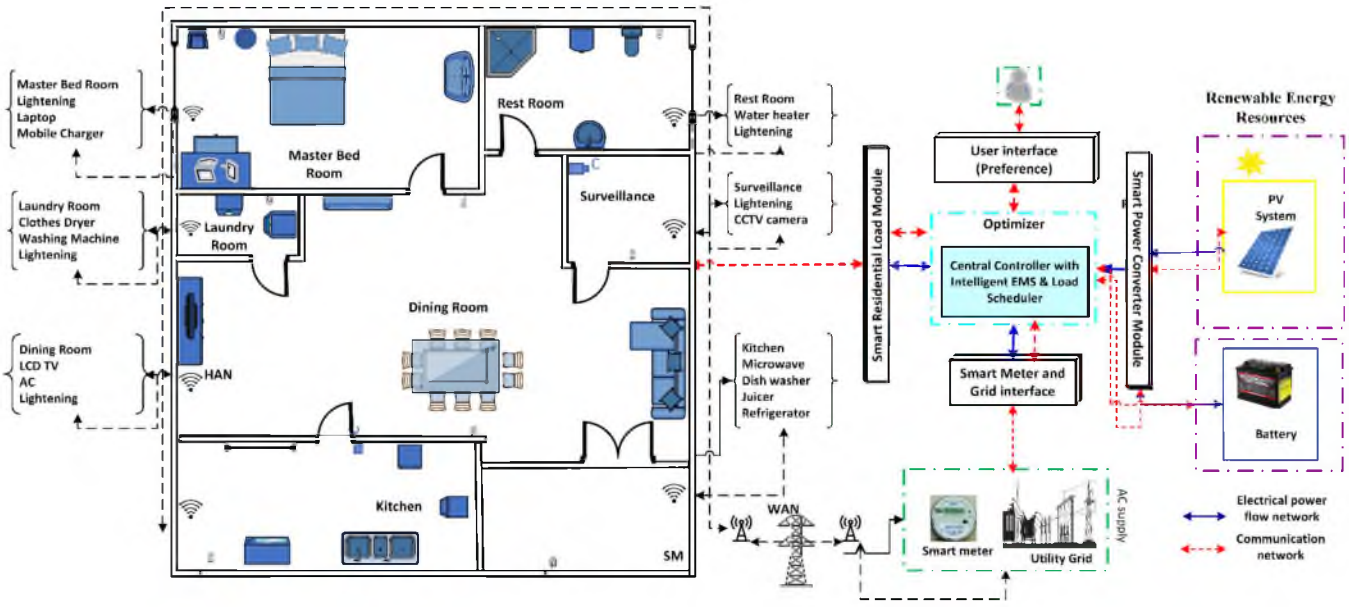

Figure 1. General configuration of the proposed SHEMS.

3. Mathematical Modeling and Parameters of the Smart Home Units

To design a smart home environment, modeling is divided into two sections: (1) modeling of RERs, which includes PV and ESS, and (2) modeling of the consumer preference-enabled system. Due to the intermittent nature of RERs, it is necessary to understand the behavioral characteristics in actual meteorological conditions of the relevant locality by modeling, numerical simulation, and evaluating the PV system. The mathematical model

of PV from [27] is considered in this paper. The technical and economical specifications and the product models of elements are also reported.

3.1. PV Module Modeling

The output power of the PV module (POW^{pv}) is mainly dependent on the sun's irradiance and ambient temperature (T^{amb}). For a time interval t, the POW^{pv} can be calculated as [11]:

$$POW^{pv} = N^{pv} \times P_r^{pv}\left(G/G^{ref}\right)\left[1 + T^{cof}\left(T^c - T^{ref}\right)\right] \quad (1)$$

where N^{pv}, P_r^{pv}, G, G^{ref}, T^{cof}, T^c, and T^{ref} represent the estimated number of required PV modules at each iteration of the sizing process [27], the rated electrical power capacity of the PV module (W), the irradiance of the sun (W/m^2), the value of solar irradiance at reference conditions taken as 1000 (W/m^2), temperature coefficient of PV module (generally rated as -3.7×10^{-3} °C^{-1} for mono- and poly-crystalline silicon [28]), the cell temperature, and the temperature at benchmark performance testing conditions (usually taken as 25 °C), respectively. The cell temperature T^c can be calculated by [29]:

$$T^c = T^{amb} + \left(\left(\left(T^{noct} - 20\right)/800\right) \times G\right) \quad (2)$$

where T^{noct} symbolizes a crucial PV module performance parameter termed nominal operating cell temperature (°C) and is defined as the temperature achieved by open-circuited cells in a module when subjected to specific conditions. The PV manufacturers generally provide this value as part of their product specification data. In this work, a 36-cell monocrystalline solar module (STP275S-20/Wem) with a power rating of 275 W is taken into consideration [28]. Table 2 provides the economic and technical aspects of the considered PV module.

Table 2. Economic and technical characteristics of RER components.

	Parameters (Units)	Values
1.	PV Module (STP275S-20/Wem)	
	Installation charges ($/W$_p$)	0.5
	Maintenance charges ($/year)	20
	Replacement charges ($/year)	0
	Regulator charges ($)	1500
	Rated power at STC (W)	275
	Module efficacy (%)	16.9
	Temperature coefficient T^{cof} (1/°C)	-3.7×10^{-3}
	Nominal operating cell temperature T^{noct} (°C)	45 ± 2
	Lifetime (years)	25
2.	Battery module	
	Installation charges ($/kW h)	180
	Maintenance charges ($/year)	5
	Replacement charges ($/year)	180
	O&M charges ($/year)	5
	Nominal voltage (V)	12
	Rated capacity (kW h)	1
	Hourly self-discharge rate σ (%/hour)	0.007
	Maximum SOC (%)	100
	Minimum SOC (%)	30
	Maximum DOD (%)	70
	Lifetime (years)	5
3.	Inverter	
	Installation charges ($)	2500
	Efficiency (%)	92
	Lifetime (years)	15

Table 2. *Cont.*

	Parameters (Units)	Values
4.	Economic indices	
	Inflation rate (%)	3
	Project life (years)	25

3.2. ESS Module Modeling

A battery bank is necessary to store the energy generated by intermittently available solar energy. Therefore, it is also required to know the state of charge (SOC) of the battery bank [30]. When the power generation from the PV module (POW^{pv}) is more than the consumption, the battery is considered to be in the charging mode. For instance t, the amount of charge, can be calculated by the following equation:

$$E_{BT}(t) = E_{BT}(t-1)\cdot(1-\sigma) + \left(POW^{pv}\cdot\eta_{inv} - \frac{P_l(t)}{\eta_{inv}}\right)\cdot\eta_{BT} \quad (3)$$

where σ, η_{BT}, and η_{inv} represent the self-discharge percentage (taken as 0.007%/h [31]), battery charging/discharging efficacy (rated as 85% for either case [32]), and efficiency of the inverter, respectively. For the case where power generation from the PV module is insufficient to meet the demand, the battery is considered to be in discharging mode, and the corresponding amount of charge is calculated as:

$$E_{BT}(t) = E_{BT}(t-1)\cdot(1-\sigma) + \left(\frac{P_l(t)}{\eta_{inv}} - POW^{pv}\cdot\eta_{inv}\right)/\eta_{BT} \quad (4)$$

The battery can meet the load demand with the proviso that $SOC(t)$ is more than the minimum SOC ($\underline{SOC}$). Likewise, surplus PV power generation can be used to charge the battery module to the point where $SOC(t)$ is equal to the maximum SOC ($\overline{SOC}$). The load demand along with the preferred autonomy day (AD) are taken into consideration to estimate the battery capacity (B_{cap}) in Ampere-hour (Ah) [33]:

$$B_{cap} = \frac{AD \cdot E_L}{\eta_{inv} \times \eta_{BT} \times DOD \times V_S} \quad (5)$$

where E_L, V_S, and DOD denote mean daily energy demand, system voltage (assumed as 48 V), and battery's depth of discharge, representing the battery percentage that has been discharged with respect to battery capacity, respectively. Equation (6) estimates the number of batteries connected in series (nBT_{ss}), while Table 2 provides the specifications of the battery module under consideration.

$$nBT_{ss} = \frac{B_{cap}}{Max\_P_s} \quad (6)$$

where Max_P_s denotes the maximum count of parallel strings. The number of batteries in the individual series string (nBT'_{ss}) is calculated by:

$$nBT'_{ss} = \frac{V_B}{V_s} \quad (7)$$

where V_B, denotes the voltage of the battery bank. The desired aggregate quantity of batteries is computed by:

$$TnB = nBT_{ss} \times nBT'_{ss} \quad (8)$$

The smart home utilizes deep-cycle lead-acid batteries based on ESS, which are widely employed owing to their affordability, wide availability, modest performance, and life cycle properties [34].

3.3. Consumer Preference and Comfort-Enabled System Modeling

A smart home typically consists of various electrical and electronic devices installed in different residence sections. The smart home under consideration contains six portions, each having different smart devices which provide varying satisfaction levels to the consumer during the course of the day. Furthermore, the power required by each device also varies according to its functionality. Table 3 lists the type and section of these devices, their quantity, and energy ratings. The evaluation of the cost of use is based on the energy tariff acquired from the energy provider in Quetta, Pakistan.

Table 3. Load cost table of a typical electricity consumer.

No.	Sections	Appliances	Quantity	Power Unit Rating (kW)	Total Power Unit Rating (kW)
1	Laundry room	Washing machine	1	0.7	0.7
2		Lightening	1	0.03	0.06
3	Dining room	Lightening	3	0.02	0.1
4		LCD TV	1	0.15	0.15
5		Computer	1	0.1	0.1
6		AC	1	1.2	1.2
7	Bathroom	Lightening	1	0.02	0.04
8	Kitchen	Juicer	1	0.4	0.4
9		Microwave oven	1	1.5	1.5
10		Refrigerator	1	0.4	0.4
11		Lightening	3	0.03	0.09
12	Master bedroom	Laptop	1	0.06	0.06
13		Lightening	3	0.02	0.1
14		AC	1	1.2	1.2
15		Mobile	1	0.006	0.006
16	Security room	CCTV Camera	3	0.009	0.027
17		Lightening	2	0.02	0.16

Consumers usually allocate a limited budget for their electricity demands. Therefore, a scheduling algorithm's primary goal is to regulate appliance usage patterns to achieve the highest consumer satisfaction level with a minimum budget. Consumer satisfaction provides a comparative view of the consumer's expectations versus their perceived experience. Consumer satisfaction tends to get higher when the scheduling algorithm schedules the appliances closer to consumer preferences.

Consumers can assign different preference values to individual devices for each hour of the day. To achieve the goals of this work, the following assumptions regarding preference are made:

(1) Preference is a quantifiable value, and its numerical analysis is possible.
(2) Preference is fuzzy in nature, implying that it has a progressive transition among the lowest (pr = 0) and highest (pr = 1) preference values.
(3) Preference is both comparable and relatable. Two modes of relativities are defined: time-based relativity and device-based relativity.

In time-based relativity, the device's preferences, which are assigned for different time periods of the day, vary according to time. For instance, Table 4 provides time-based preferences, ranging from 0 to 1, which are indexed row-wise (viz. horizontally) by the consumer. On the other hand, in device-based relativity Table 5, the consumer indexes the data column-wise (viz. vertically) for hourly time slots over 24 h. This consumer preference table compares a particular device's preference to other devices for a specific hour. Consumer preference tables (Tables 4 and 5) were acquired from middle-class residents living in Quetta, Pakistan. For example, Tables 4 and 5 show the consumer preferences for the summer season, where consumers require excessive air conditioning compared to other seasons. Consumer preference for other seasons was also acquired and considered for this work.

During the pandemic, more people are forced or opting for home office, resulting in commutation exclusion. Consequently, morning residential energy demand peaks have been postponed, and residential energy usage at noon has increased by 23% to 30% [29]. This changed daily routine is also reflected in the consumer preference tables (Tables 4 and 5).

Time- and device-based preferences are taken into account to determine the absolute satisfaction, '$\mu_{s(k)}(\tau_i)$' and is calculated by [35]:

$$\mu_{s(k)}(\tau_i) = \sqrt{\frac{\left(\rho_k^T(\tau_i)\right)^2 + \left(\rho_k^D(\tau_i)\right)^2}{2}} \; \forall \, i = [1, 24] \tag{9}$$

where time and device-based preferences of appliance k at instance i are represented by '$\rho_k^T(\tau_i)$' and '$\rho_k^D(\tau_i)$', respectively. Table 6 shows the absolute consumer satisfaction table derived from time and device-based preferences for summer. Figure 2 illustrates the seasonal absolute satisfaction levels.

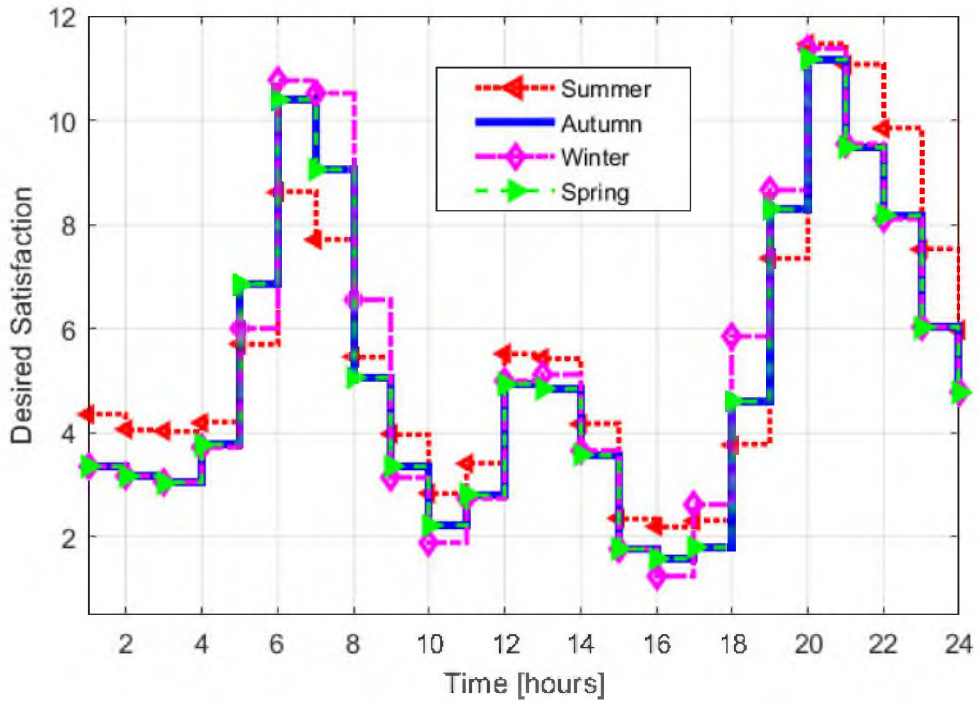

Figure 2. Daily absolute satisfaction values for the four seasons of the year.

Table 4. Time-based consumer preference table for summer.

Sections	Appliances	1	2	3	4	5	6	7	8	9	10	11	12	13	14	15	16	17	18	19	20	21	22	23	24
Laundry room	W.Machine	0	0	0	0	0.2	0.8	0.5	0	0	0	0	0	0	0	0	0	0	0	0	0	0	0	0	0
	Lighting	0	0	0	0.1	0.2	1	1	0	0	0	0.1	0.2	0.1	0.1	0	0	0	0	0	0	0	0	0	0
Living room	Lighting	0	0	0	0	0.1	0.1	0.1	0.1	0.1	0	0.1	0.1	0.1	0.1	0	0	0.1	0.1	0.5	1	1	0.9	0.5	0.2
	LCD TV	0	0	0	0	0	0.4	0.3	0.1	0	0	0.1	0.2	0.1	0.1	0	0	0.2	0.4	0.7	0.8	1	1	0.7	0.5
	Computer	0	0	0	0	0.1	0.5	0.8	1	1	1	1	0.8	0.8	0.8	1	1	0.9	0.5	0.1	0	0	0	0	0
	AC	0	0	0	0	0.1	0.5	0.8	1	1	1	0.5	0.5	0.5	0.5	0	0	0.9	0.5	0.5	0.8	1	0.8	0.9	0.2
Bathroom	Lighting	0	0	0	0	0.2	0.1	0.1	0	0	0	0	0	0	0	0	0	0	0.1	0.5	0.9	1	0.8	0.5	0.3
Kitchen	Juicer	0	0	0	0	0.1	0.2	1	0.8	0.3	0	0.2	1	0.8	0.3	0	0	0	0.1	0.2	1	0.8	0.3	0	0
	Oven	0	0	0	0	0.1	0.3	0.9	1	0.5	0	0.3	0.9	1	0.5	0	0	0	0.2	0.2	1	0.8	0.3	0	0
	Refrigerator	0.5	0.5	0.5	0.5	0.5	0.5	1	0.7	0.4	0	0.5	1	0.7	0.4	0	0	0.1	0.9	1	0.5	0.3	0.2	0.1	0.1
	Lighting	0	0	0	0	0.2	0.1	0	0	0	0	0.1	0.1	0.1	0.1	0	0	0	0	0.5	1	0.8	0.6	0.2	0
M.bedroom	Laptop	0	0	0	0	0.1	0.3	0.1	0	0	0	0.1	0.2	0.2	0.1	0	0	0	0.1	0.5	0.5	0.8	1	0.8	0.7
	Lighting	0	0	0	0	0.5	0.1	0	0	0	0	0	0	0	0	0	0	0	0	0.1	0.5	0.8	0.9	1	0.2
	AC	1	1	1	1	0.8	0.5	0.1	0	0	0	0	0	0	0	0	0	0	0	0.1	0.5	0.8	0.9	1	1
	M.Charger	1	0.7	0.5	0.4	0.3	0.3	0.2	0.1	0	0	0	0	0	0	0	0	0	0	0.1	0.2	0.3	0.4	0.5	0.8
Security room	CCTV	1	1	1	0.9	0.8	0.8	0.5	0.2	0	0	0	0	0	0	0	0	0	0	0.2	0.5	0.7	0.8	1	1
	Lighting	1	1	1	0.9	0.5	0	0	0	0	0	0	0	0	0	0	0	0	0	0	0.5	0.7	0.8	1	1

Table 5. Device-based consumer preference table for summer.

Sections	Appliances	1	2	3	4	5	6	7	8	9	10	11	12	13	14	15	16	17	18	19	20	21	22	23	24
Laundry room	W.Machine	0	0	0	0	0.2	1	0.5	0.1	0	0	0	0.1	0	0	0	0	0	0.1	0.4	0.8	0.5	0.1	0	0
	Lighting	0	0	0	0.1	0.2	0.1	0	0	0	0	0	0	0	0	0	0	0	0	0.2	0.2	0.2	0.4	0	0
Living room	Lighting	0	0	0	0	0.1	0.3	0	0	0.1	0.1	0.1	0.1	0.1	0.1	0.1	0.1	0.1	0.1	0.5	0.5	1	0.9	0.7	0.2
	LCD TV	0	0	0	0	0	0	0.3	0.3	0	0	0.1	0.2	0.2	0.1	0	0	0.2	0.5	0.7	0.8	1	1	0.7	0.3
	Computer	0	0	0	0	0.1	0.3	0.5	0.8	1	1	1	0.9	0.9	1	1	1	1	0.8	0.1	0	0	0	0	0
	AC	0	0	0	0	0.1	0.3	0.8	1	1	1	1	0.9	0.8	0.8	0.8	0.8	0.9	0.9	0.9	0.5	0.8	0.9	0.5	0.2
Bathroom	Lighting	0.1	0.1	0.1	0.1	0.3	0.9	0	0	0	0	0	0	0	0	0	0	0	0	0.2	0.5	0.1	0.3	0.2	0.1
Kitchen	Juicer	0	0	0	0	0.2	0.5	1	0.1	0.1	0	0.2	0.8	1	0.1	0	0	0	0	0.5	1	0.2	0.1	0	0
	Oven	0	0	0	0	0.3	0.6	1	0.1	0.1	0	0.2	0.8	1	0.1	0	0	0	0	0.6	1	0.2	0.1	0	0
	Refrigerator	0.5	0.5	0.5	0.3	0.3	0.6	0.4	0.1	0.1	0.1	0.2	0.3	0.5	0.4	0.1	0.1	0.1	0.9	1	1	1	1	1	0
	Lighting	0.5	0	0	0.1	0.2	0.1	0.1	0	0	0	0	0	0	0	0	0	0	0	0.3	0.5	1	1	0	0

Table 5. *Cont.*

Sections	Appliances	1	2	3	4	5	6	7	8	9	10	11	12	13	14	15	16	17	18	19	20	21	22	23	24
M.bedroom	Laptop	0.1	0.2	0	0	0	0.4	0.2	0.1	0	0	0	0	0	0	0	0	0	0.1	0.1	0.1	0.2	1	0.8	0.7
	Lighting	0.2	0.1	0.1	0.2	0.5	0.3	0	0	0	0	0	0	0	0	0	0	0	0	0.1	0.1	0.3	0.3	1	0.4
	AC	1	0.8	1	0.8	1	0.5	0.1	0	0	0	0	0	0	0	0	0	0	0	0.1	0.5	0.8	0.9	1	1
	Mobile	1	0.9	0.7	0.3	0.3	0.1	0.1	0	0	0	0	0	0	0	0	0	0	0	0.1	0.5	0.5	0.6	0.2	0.9
Security room	CCTV	1	1	1	1	1	0.8	0.1	0.2	0	0	0	0	0	0	0	0	0	0.2	0.1	0.3	0.5	0.5	0.8	1
	Lighting	1	1	1	1	0.5	0.3	0	0	0	0	0	0	0	0	0	0	0	0	0.1	0.2	0.4	0.5	0.7	1

Table 6. Absolute consumer satisfaction table derived from consumer's time and device-based preferences for summer.

Sections	Appliances	1	2	3	4	5	6	7	8	9	10	11	12	13	14	15	16	17	18	19	20	21	22	23	24
Laundry room	W.Machine	0.0	0.0	0.0	0.0	0.2	0.9	0.5	0.1	0.0	0.0	0.0	0.1	0.0	0.0	0.0	0.0	0.0	0.1	0.3	0.6	0.4	0.1	0.0	0.0
	Lighting	0.0	0.0	0.0	0.1	0.2	0.7	0.7	0.0	0.0	0.0	0.1	0.1	0.1	0.1	0.0	0.0	0.0	0.0	0.1	0.1	0.1	0.3	0.0	0.0
Living room	Lighting	0.0	0.0	0.0	0.0	0.1	0.2	0.1	0.1	0.1	0.1	0.1	0.1	0.1	0.1	0.1	0.1	0.1	0.1	0.5	0.8	1.0	0.9	0.6	0.2
	LCD TV	0.0	0.0	0.0	0.0	0.0	0.3	0.3	0.2	0.0	0.0	0.1	0.2	0.2	0.1	0.0	0.0	0.2	0.5	0.7	0.8	1.0	1.0	0.7	0.4
	Computer	0.0	0.0	0.0	0.0	0.1	0.4	0.7	0.9	1.0	1.0	1.0	0.9	0.9	0.9	1.0	1.0	1.0	0.7	0.1	0.0	0.0	0.0	0.0	0.0
	AC	0.0	0.0	0.0	0.0	0.1	0.4	0.8	1.0	1.0	1.0	0.8	0.7	0.7	0.7	0.6	0.6	0.9	0.7	0.7	0.7	0.9	0.9	0.7	0.2
Bathroom	Lighting	0.1	0.1	0.1	0.1	0.3	0.6	0.1	0.0	0.0	0.0	0.0	0.0	0.0	0.0	0.0	0.0	0.0	0.1	0.4	0.7	0.7	0.6	0.4	0.2
Kitchen	Juicer	0.0	0.0	0.0	0.0	0.2	0.4	1.0	0.6	0.2	0.1	0.2	0.9	0.9	0.2	0.0	0.0	0.0	0.1	0.4	1.0	0.6	0.2	0.0	0.0
	Oven	0.0	0.0	0.0	0.0	0.2	0.5	1.0	0.7	0.4	0.0	0.3	0.9	1.0	0.4	0.0	0.0	0.0	0.1	0.4	1.0	0.6	0.2	0.0	0.0
	Refrigerator	0.5	0.5	0.5	0.4	0.4	0.6	0.8	0.5	0.3	0.1	0.4	0.7	0.6	0.4	0.1	0.1	0.1	0.9	1.0	0.8	0.7	0.7	0.7	0.1
	Lighting	0.4	0.0	0.0	0.1	0.2	0.1	0.1	0.0	0.0	0.0	0.1	0.1	0.1	0.1	0.0	0.0	0.0	0.0	0.4	0.8	0.9	0.8	0.1	0.0
M.bedroom	Laptop	0.1	0.1	0.0	0.0	0.1	0.4	0.2	0.1	0.0	0.0	0.1	0.1	0.1	0.1	0.0	0.0	0.0	0.1	0.4	0.4	0.6	1.0	0.8	0.7
	Lighting	0.1	0.1	0.1	0.1	0.5	0.2	0.0	0.0	0.0	0.0	0.0	0.0	0.0	0.0	0.0	0.0	0.0	0.0	0.1	0.4	0.6	0.7	1.0	0.3
	AC	1.0	0.9	1.0	0.9	0.9	0.5	0.1	0.0	0.0	0.0	0.0	0.0	0.0	0.0	0.0	0.0	0.0	0.0	0.1	0.5	0.8	0.9	1.0	1.0
	Mobile	1.0	0.8	0.6	0.4	0.3	0.2	0.2	0.1	0.0	0.0	0.0	0.0	0.0	0.0	0.0	0.0	0.0	0.0	0.1	0.4	0.4	0.5	0.4	0.9
Security room	CCTV	1.0	1.0	1.0	1.0	0.9	0.8	0.4	0.2	0.0	0.0	0.0	0.0	0.0	0.0	0.0	0.0	0.0	0.2	0.4	0.5	0.7	0.8	0.9	1.0
	Lighting	1.0	1.0	1.0	1.0	0.5	0.2	0.0	0.0	0.0	0.0	0.0	0.0	0.0	0.0	0.0	0.0	0.0	0.0	0.4	0.5	0.6	0.8	0.9	1.0

4. Climatological Conditions and Energy Demand of the Study Location

To accurately design and evaluate the capabilities of the proposed algorithm, accurate climatological data is required to emulate real-world conditions while performing different calculations for this work. As far as this study is concerned, the actual climatological data for the year 2017 of Quetta, Pakistan, was used. This data was acquired from World Bank via ENERGYDATA.info [36]. Quetta city has GPS coordinates of 30°10′59.7720″ N and 66°59′47.2272″ E. This region has plenty of sunlight and low cloud cover throughout the year. The irradiance and temperature are measured using a solar station which records these values in 10 min time intervals throughout the year. The measured air temperature and solar irradiance of the selected location are shown in Figure 3. This annual climatological data was used as input for the calculations performed in this study. Figure 3 also shows the annual residential load at the study location.

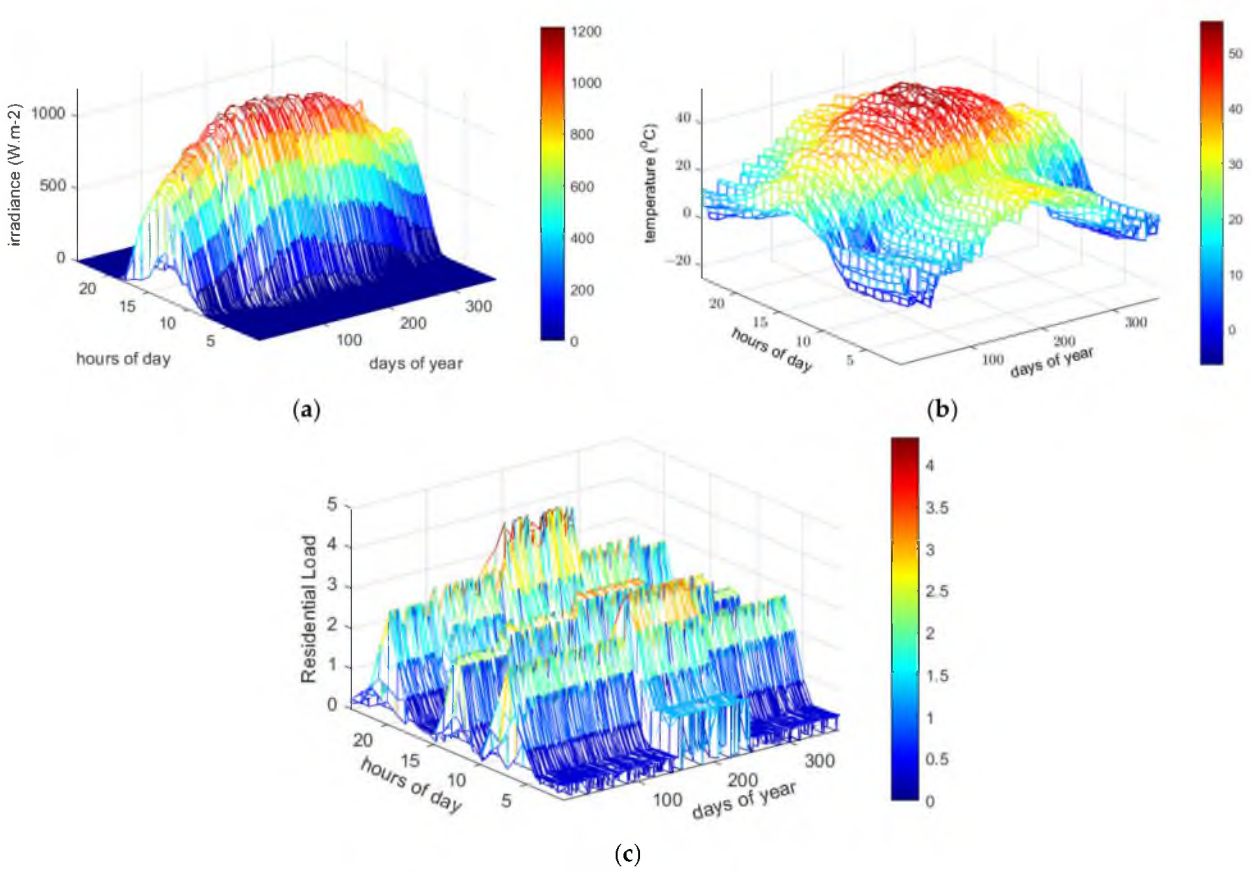

Figure 3. Graphs showing the distribution of annual (**a**) solar irradiance, (**b**) air temperature, and (**c**) residential load at Quetta, Pakistan.

5. Energy Management System for Integration of RER and ESS

The intermittency (seasonal/diurnal) and volatility of renewables exclude the possibility of exclusively relying on RERs for catering to the energy demand, which adds to the complexity of designing an EMS. The EMS optimally executes different modes of energy flow in light of consumer-assigned satisfaction levels. P_l, POW^{pv}, SOC, $\underline{SOC}$, and $\overline{SOC}$ form the basis for the definition of primary strategies. The algorithm uses sub-system models defined in Section 3 to calculate the energy production from RERs by considering the initial SOC value and regional meteorological data. Subsequently, the MGWASA-based algorithm determines the optimum switching pattern based on this data and consumer input (consumer satisfaction). Our work defines the following four primary operation modes to implement the proposed SHEMS:

- Mode I: Provided adequate solar energy is available to cater to the energy demand, surplus energy is used to charge the battery bank, given that the battery is not fully charged.
- Mode II: The surplus solar energy is exported to the grid as long as the energy produced by the PV can fulfill the residential load demand and the battery bank is fully charged.
- Mode III: In the case where the energy produced by the solar cannot meet the load demand, the energy available in the battery bank is utilized to cater to the remaining load demand.
- Mode IV: When the load demand is more than the energy provided by PV and battery bank, then the remaining load demand is catered by the energy imported from the grid.

The flowchart of the implemented algorithm for SHEMS, involving the operation modes defined above, is drawn in Figure 4.

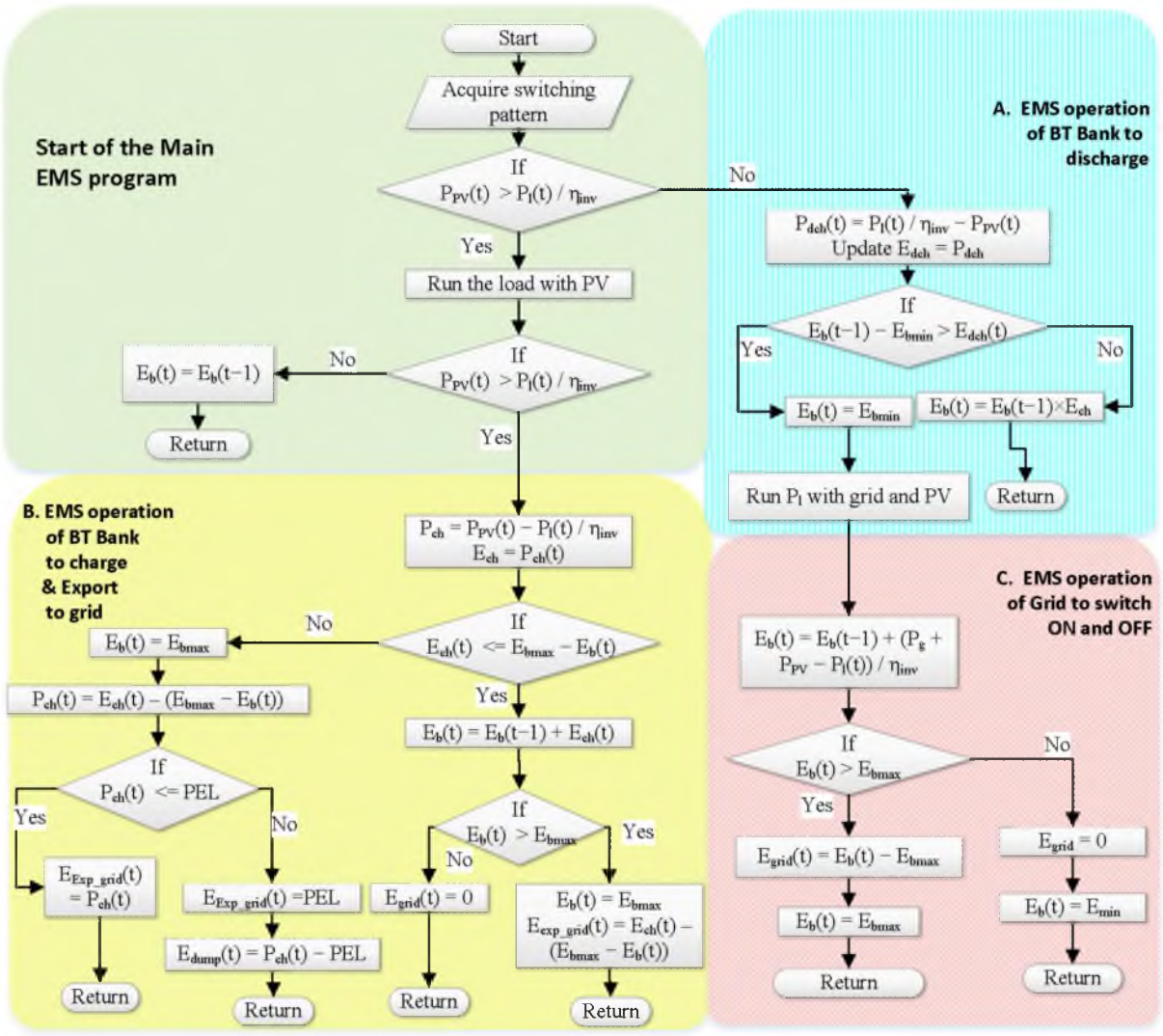

Figure 4. The flowchart of the implemented EMS algorithm describes various modes of operation.

The EMS (Section 5) and preference-enabled system of the smart home (Section 3.3) is combined with the application of real-time data in the MGWASA to obtain a set of appliance scheduling solutions. The detail of the proposed algorithm is provided in the next section.

6. Proposed Multi-Criteria Grey Wolf Accretive Satisfaction Algorithm (MGWASA)

Even though the GWO algorithm is relatively new, its shortcomings have limited its usage to single optimization problems. Recently, a few variants of GWO have been introduced to deal with multi-objective problems [37]. It is also not feasible to directly employ the multi-objective GWO algorithm to handle multi-objective feature selection or load scheduling problems because it was originally designed to handle continuous optimization tasks. However, with the addition of the squashing activation function, a binary MGWO variant was proposed to tackle the above-mentioned tasks [38,39]. This binary MGWO is combined with the preference-based smart home model and EMS to develop an MGWASA. The binary population represents the scheduling patterns of the appliances. The equation formulated for updating the position is given as:

$$x_d^{t+1} = \begin{cases} 1 & if\ squash\left(\frac{x_1+x_2+x_3}{3}\right) \geq rand \\ 0 & otherwise \end{cases} \tag{10}$$

where x_d^{t+1} represents the position amended according to binary, d represents dimension, t is the iteration, and $rand$ indicates a random number extracted from distribution uniform $\in [1, 0]$. While x_1, x_2, and x_3 denote positions of alpha, beta, and gamma wolves, respectively. $squash(a)$, x_1, x_2, and x_3 are given as:

$$squash(a) = \frac{1}{1 + e^{-10(x-0.5)}} \tag{11}$$

$$x_1^d = \begin{cases} 1 & \left(x_\alpha^d + bstep_\alpha^d\right) \geq 1 \\ 0 & otherwise \end{cases} \tag{12}$$

$$x_2^d = \begin{cases} 1 & \left(x_\beta^d + bstep_\beta^d\right) \geq 1 \\ 0 & otherwise \end{cases} \tag{13}$$

$$x_3^d = \begin{cases} 1 & \left(x_\gamma^d + bstep_\gamma^d\right) \geq 1 \\ 0 & otherwise \end{cases} \tag{14}$$

$$bstep_{\alpha,\beta,\gamma}^d = \begin{cases} 1 & if\ cstep_{\alpha,\beta,\gamma}^d \geq rand \\ 0 & otherwise \end{cases} \tag{15}$$

where $cstep_{\alpha,\beta,\gamma}^d$ represents continuous step size value and is expressed as

$$cstep_{\alpha,\beta,\gamma}^d = \frac{1}{1 + e^{-10(A_1^d D_{\alpha,\beta,\gamma}^d - 0.5)}} \tag{16}$$

Figure 5 summarizes the process of the proposed MGWASA. Time and device-based preference tables, appliance power rating tables, irradiance, and temperature data are taken as input to the algorithm. Irradiance and temperature data are used to estimate the PV power production, whereas time and device-based preference tables form the basis for the satisfaction table. All of these values are further required to formulate the multi-criteria objective function.

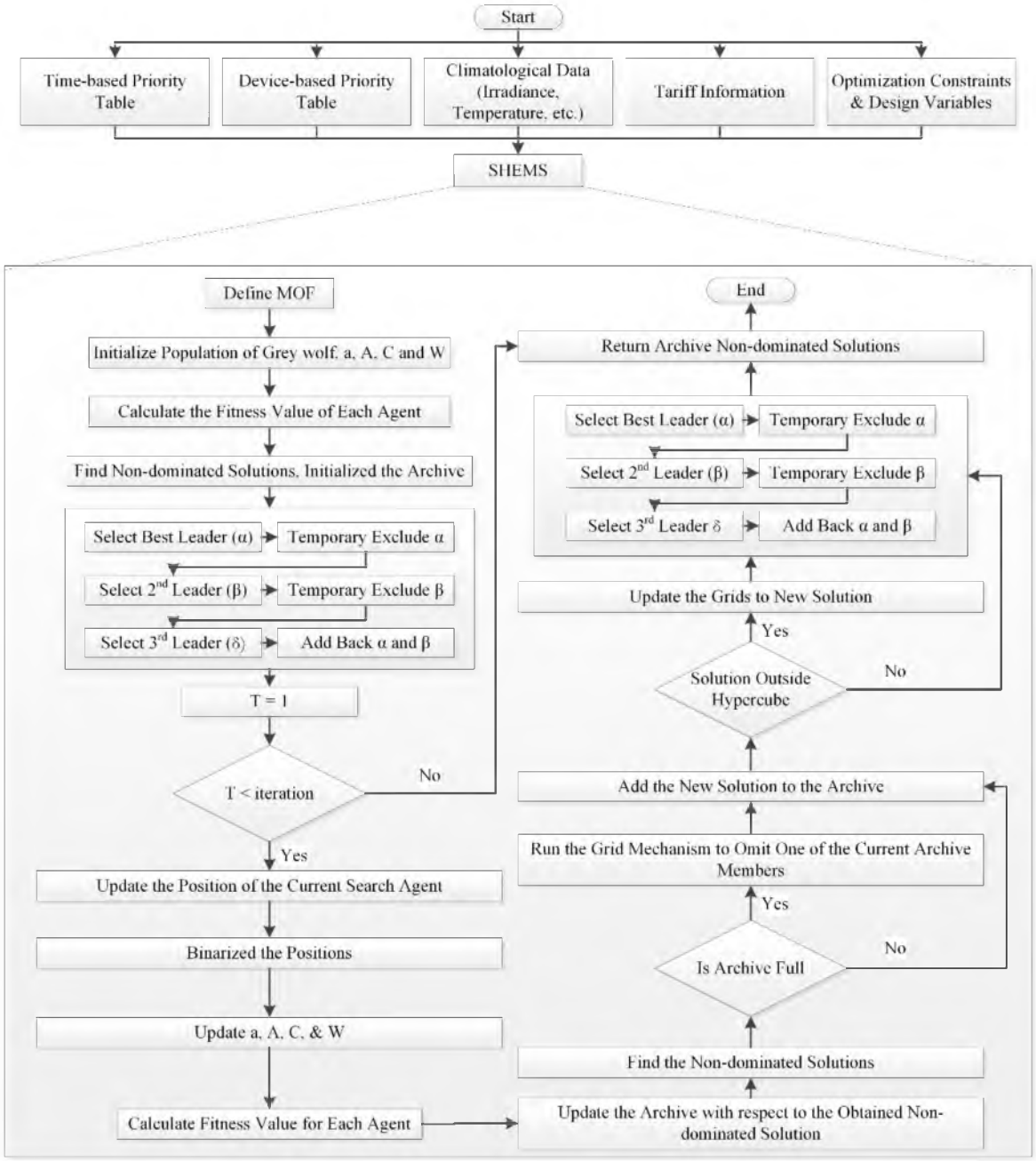

Figure 5. Flowchart of the proposed MGWASA.

6.1. Multi-Objective Problem Formulation of DSM

The proposed multi-criteria device scheduling in the smart home consists of formulating an optimization problem that constitutes the objective function, constraints, scheduling pattern, and state-of-the-art meta-heuristic optimization algorithm described in the subsequent sub-section.

6.1.1. Multi-Criteria Objective Function

Three main objective functions are of great importance in the design of a smart home, namely, the economic aspect objective (cost), the technical aspect objective (reliability), and the comfort aspect (consumer satisfaction). These objectives conflict with each other; for example, cost increases exponentially by increasing reliability and consumer satisfaction. Similarly, by decreasing the reliability and comfort level, cost decreases. Intrinsically, sets of non-dominated objective functions known as the Pareto front are preferred to be calculated.

The cost of energy which covers the financial aspect, and consumer satisfaction which covers the comfort aspect, are the two objective functions considered for minimization. Whereas the reliability of the system is improved by the integration of RERs into the system. The mathematical formulation of this constrained optimization problem is described in the following.

Cost per Unit Satisfaction Index ($C_{s\_index}(\$)$)

Energy cost is related to the satisfaction level of the consumer. $C_{s\_index}(\$)$ is the measure of total consumer expenditure (TU_{exp}) related to the derived consumer satisfaction (μ_s) as shown in Equation (19)). TU_{exp} represents the total consumer energy cost, which is the product of total energy consumption (TEC) and energy tariff when the load is only powered by the utility grid, while the TU_{exp} is changed when RER is integrated into the system. The cost of PV, battery, and inverter is also added in the TU_{exp} along with the cost of the load run by the utility grid as shown in Equation (11)). The contribution of the utility grid is based on the available amount of PV energy and SOC set point. TEC is computed by summation of the total operating time (TOT) of all the appliances with the specified power rating (PR).

$$Obj(C_{s\_index}(\$)) = \min\ (C_{s\_index}(\$) \tag{17}$$

$$C_{s_{index}}(\$) = \frac{TU_{exp}(\$)}{\mu_s} \tag{18}$$

$$TU_{exp} = \begin{matrix} TEC \times UT \quad or \\ Grid_E \times UT + C_{PV} + C_{ESS} \end{matrix} \tag{19}$$

$$C_{PV} = \frac{(C_{WP} \times P_C \times N^{PV}) + C_{REG}}{LS_{PV}} + C_{OMPV} \times N^{PV} \tag{20}$$

$$C_{ESS} = \frac{C_{kWB} \times TBC}{LS_{BAT}} + C_{OMBAT} + \frac{C_{inv}}{LS_{inv}} \tag{21}$$

$$\mathrm{TEC} = \sum_{\mathrm{n=A}}^{\mathrm{Z}} (\mathrm{TOT_n} \times \mathrm{TPR_n}) \tag{22}$$

where, C_{WP}, P_C, N^{PV}, C_{REG}, C_{OMPV}, and LS represent cost per unit watt, panel capacity, number of panels, regulator cost, yearly PV O&M cost, and lifespan of the module. The yearly cost of the battery is calculated in Equation (21) where C_{kWB}, TBC, C_{OMBAT} and LS, C_{inv} represents the cost per unit kilo watt, total battery capacity, operational and maintenance cost, the lifespan of the module, and inverter cost.

Consumer Satisfaction or Percentage Satisfaction

The energy cost is generally directly proportional to the consumer's comfort or satisfaction level. However, a clear relationship between consumer satisfaction and cost must be established. For this purpose, the satisfaction level is quantified by the consumer's time and device-based preferences. A mathematical model is created that relates consumer satisfaction with energy cost. The second objective of the problem is to maximize consumer satisfaction; the formulation of consumer satisfaction is given in Equation (24).

$$Obj(\mu_s\ ) = \max\ (\mu_s) \tag{23}$$

$$\mu_{s(k)}(\tau_i) = \sqrt{\frac{(\rho_k^T(\tau_i))^2 + (\rho_k^D(\tau_i))^2}{2}} \tag{24}$$

$$S_{desired} = \sum_{\mathrm{h=1}}^{24} \sum_{i=A}^{\mathrm{Z}} \mu_{s(i)}(\tau_\mathrm{h}) \tag{25}$$

$$\%S = \mathrm{S_{achieved}}\ /\mathrm{S_{desired}} \tag{26}$$

6.1.2. Constraints

Constraints related to the optimization of the objective function are as follows:

I. Constraint of idle load

If interval $[\beta_l,\eta_l]$ does not include t, then the scheduling vector $s_l(t)$, which represents the status of load in the t^{th} scheduling interval must be zero.

$$s_l(t) = 0,\ t < \beta_l\ \forall l\ \in SL \tag{27}$$

$$s_l(t) = 0,\ t > \eta_l\ \forall l\ \in SL. \tag{28}$$

II. Constraint related to the working of the battery

A battery always exhibits a unique operating modality, defined as

$$B_c(t) + B_f(t) + B_d(t) = 1 \tag{29}$$

where $B_c(t)$, $B_f(t)$, and $B_d(t)$ represent the charging, floating, and discharging modes of operation of the battery for the interval t, respectively.

III. Constraints related to battery boundaries

The battery manufacturer defines certain maximum and minimum boundaries for battery parameters, i.e., charging and discharging power and status of the charge. These constraints are described as

$$\underline{SOC} \leq SOC \leq \overline{SOC} \tag{30}$$

$$P_{BCmin} \leq P_{BC}(t) \leq P_{BCmax} \tag{31}$$

$$P_{BDmin} \leq P_{BD}(t) \leq P_{BDmax} \tag{32}$$

where $P_{BC}(t)$ and $P_{BD}(t)$ denote the battery power while charging and discharging, respectively. The maximum and minimum power limits for charging and discharging are represented by P_{BCmax}, P_{BCmin}, and P_{BDmax}, P_{BDmin}, respectively.

IV. Constraint related to export of power

Excess power above a certain limit may cause instabilities in the utility grid. Therefore, at a certain time interval t, the exported power to the utility grid $P_E(t)$ must never exceed a limit $P_{Emax}(t)$ set by the energy provider.

$$P_E(t) \leq P_{Emax}(t) \tag{33}$$

$$P_E(t) = P_R(t) - (P_l(t) + P_B(t)) \tag{34}$$

where $P_R(t)$ represents the expected power from RER, while $P_B(t)$ is the net battery power for the interval t.

7. Simulation Results and Discussion

This part validates the devised EMS employing MGWASA via a case study comprising diverse residential loads, RER and ESS. Residential loads studied in this work are located in six different sections of the residence. Table 3 provides the electrical and economic parameters of these devices. The smart home utilizes deep-cycle lead-acid batteries based on ESS, which are widely employed owing to their affordability, wide availability, modest performance, and life cycle properties [34]. Technical specifications of the employed battery are tabulated in Table 2. A roof-mounted RER system comprising PV panels is taken into consideration in this work. The rated capacity of an individual PV panel is 0.275 kW. The electricity tariff data is taken from QESCO, the local energy provider in Quetta, Pakistan. The estimated energy production from the PV is based on the data acquired from a World Bank's financed weather monitoring station installed in Quetta region [36]. Furthermore, MATLAB® is employed to implement the MGWASA-based EMS. All the results were

obtained by numerical simulations performed on a computing system having an Intel® Core™ i5-8250U CPU with 8.00 GB RAM.

Three cases are considered for simulation to verify the proposed scheduling mechanism's efficiency. In the first case, it is assumed that the smart home does not contain RER and ESS. Therefore, MGWASA is applied to all smart home appliances powered entirely by the utility grid. On the other hand, the second case covers a smart home's full potential by integrating RER and ESS in the system alongside appliance scheduling by MGWASA. The third case also considered RER and ESS integration; however, the appliance switching pattern is taken directly from the consumer preference table without optimal appliance scheduling. For further validation, the performance of MGWASA for Case 1 and Case 2 is also compared with state-of-the-art optimization algorithms: NSGAII, MOBPSO, MOABC, and MOEA.

7.1. Size Optimization of PV and ESS in a Smart Home

Both ESS's PV modules and battery units require considerable investment. Several aspects of cost, such as investment net present cost, replacement cost, O&M cost, federal incentives, import/export of electricity, and cost related to power outages over the project's lifespan, must be considered in this regard. To efficiently utilize renewable resources and increase the proposed system's reliability, sizing is optimized using a genetic algorithm (GA), based on [40], against the annual load obtained from consumer preference. Time intervals of one hour are taken during the sizing process. Various technical and economic parameters of PV and battery units are given in Table 2. The initial investment is capped at 10 k$, while 0.3 is taken as the PV energy factor.

Furthermore, 100 and 20 are the population size and generation count for the sizing problem, respectively. The optimal sizes of PV and ESS are 9.35 kW (34 PV panels) and 11 kWh, respectively. It is worth mentioning that these optimal sizes are calculated against the consumer preference-based load demand for the entire year.

7.2. Validation of the Load Scheduling and Energy Management by MGWASA

Before performing the optimization by MGWASA, the algorithm shown in Figure 5 was executed for an entire year, covering all four seasons, to validate its long-term robustness and resilience. In this regard, the minimum allowed *SOC* value of ESS is taken as 30% resulting in a DOD of 70%. The PV module employed here consists of an array of 34 panels, providing a rated power of 9.35 kW, while the ESS has a rated capacity of 11 kWh. Figures 6 and 7 show the working mechanism of designed EMS for an entire year, as well as a few samples of each season, illustrating the switching and energy flow of and between different system components according to the load demand. Figure 7a shows that at the start of the day (00 h), the ESS (dotted blue line) is at its minimum allowable storage limit ($SOC = 30\%$). Therefore, the load demand (black dash line) is catered to by importing the power from the utility grid (brown shaded area). However, this import gradually drops and eventually goes to zero once the power production from the PV (red-shaded area) starts. After a certain time, power production from PV is more than the load demand. In this case, the surplus energy is channeled toward the ESS for charging (the green-shaded area). At noon, the ESS is completely charged ($SOC = 100\%$), and the surplus energy from PV is exported to the utility grid (grey-shaded area). In the evening, as the sun goes down, the power generation from PV is not sufficient to cater to the load demand. Therefore, the energy stored in ESS is used in synergy with PV power to meet the load demand. In the late hours of the day, when the charge of the ESS has depleted to its minimum allowable level ($SOC = 30\%$), and there exists no PV power as well, the utility grid supplies all the required power. The next day starts similarly, taking the *SOC* values from the previous day and so on.

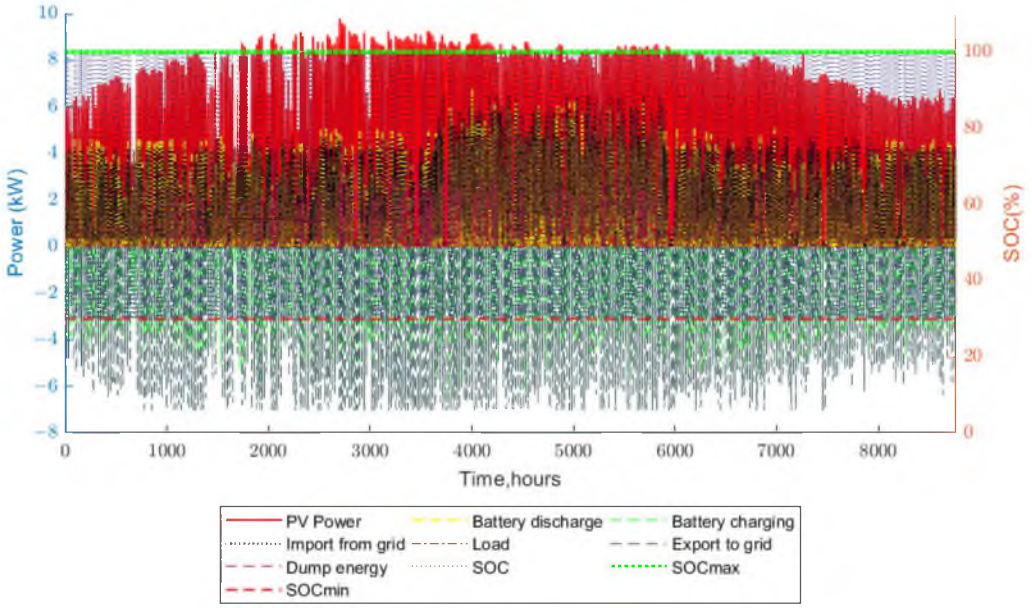

Figure 6. EMS energy mix analysis for the entire year.

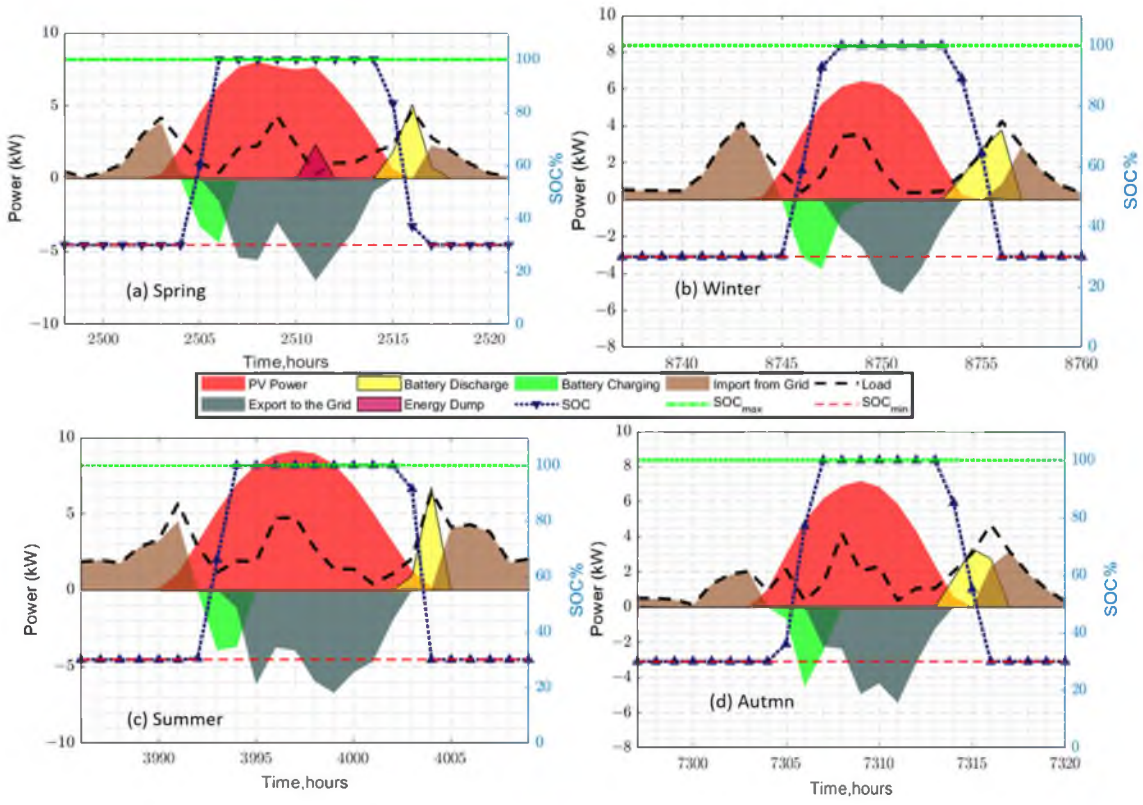

Figure 7. EMS energy mix analysis for a day of (**a**) spring, (**b**) winter, (**c**) summer, and (**d**) autumn.

Additionally, a slight dip can be observed in the PV power graph in the afternoon. This dip is attributed to variations in climatological conditions, such as passing clouds, rain, etc. However, the absence of abrupt changes in the PV power curve implies that irradiance is not disturbed by sudden fluctuations in weather conditions. Nonetheless, it can be observed from Figure 7a–d that the amount of daily PV power varies seasonally because of seasonal irradiance variations, e.g., PV power in summer is higher than in other seasons due to a higher irradiance value.

The current research work further exploits the capability of a maiden MGWASA embedded with Pareto optimal front* to optimize the smart home load scheduling. MGWASA can simultaneously and independently optimize the objective function (C_{s_index}, $\%S$), and perhaps the impact of variation in cost can only be realized by simultaneously considering both objectives. The multi-objective optimization problem is formed by a linear combination of two objectives expressed as follows:

$$Minimize\ wF_1 + (1 - w)\varnothing.PF.F_2 \tag{35}$$

Equation (35) has been applied to two conflicting nature objectives, $F_1 = C_{s\_index}$ and $F_2 = \%S$. w in Equation (35) denotes a weighting factor randomly generated in the range of (0,1). Its value is set at zero and progressively increased in the step of 0.05 up to 1. $\varnothing$ is a scaling factor chosen as 1000. The two objectives have different units in the multi-objective optimization problem; a penalty factor (PF) is considered to balance the objectives properly.

Figure 8 shows the considered utility grid tariff pricing scheme for each season. Tariff prices show seasonal variations with increased prices in the evenings. This peak time variation is in accordance with the sunset timing of the case study location.

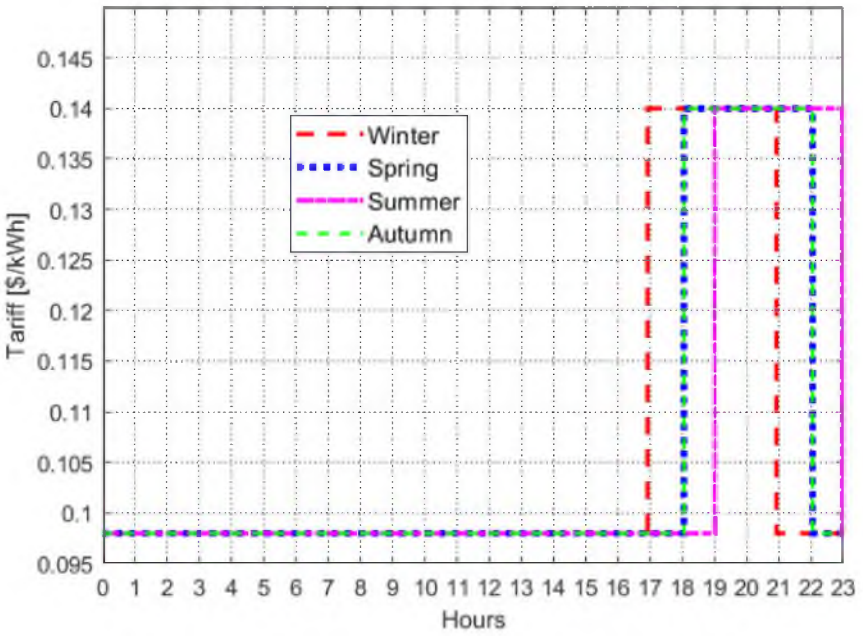

Figure 8. Tariff used for the simulation of MGWASA.

Six different test cases, each corresponding to 17 appliances in a smart home, are considered to demonstrate the proposed approach. In Case 1, MGWASA is applied only on the appliances for optimal scheduling without taking advantage of EMS. While in Case 2, EMS is also integrated into optimal scheduling to see the impact of renewable resources and energy storage on the cost and consumer satisfaction. Case 3 and Case 4 are related to the ideal load directly extracted from consumer satisfaction. Initially, the ideal load is run by the utility grid then the effect of EMS is considered. Lastly, Case 5 and Case 6 are based on the random load, also called base load profile, without and with EMS, respectively. MGWASA runs for five iterations with a population size of 1000, and the solution obtained for the smart home offers scheduling load and RER sequencing. The results offer a set of optimum trade-off solutions (non-dominated solutions) in the Pareto front, giving the decision-makers several options. The results of the above-stated cases are shown and discussed in the subsequent sub-sections.

7.2.1. Case 1: Appliance Scheduling Using MGWASA without Integration of EMS

In this case, the load scheduling problem is solved by employing MGWASA without integrating RER and ESS. Figure 9 shows the process of grey wolves hunting for their prey. In every iteration, 1000 grey wolves are approaching the best possible Pareto-front solutions and adding the best solutions in the archive shown with the red markers. In the shown example, MGWASA is tested for a day of the summer season. After meeting the termination criteria, which is the maximum number of iterations, MGWASA produces a final set of non-dominated solutions of scheduling patterns which gives the consumer a range of solutions to opt for according to the consumer budget. Non-dominated solutions of two objective functions are shown in Figure 10. The maximum obtained $\%S$ is 92.44% with the 0.056\$ C_{s_index}, and the minimum $\%S$ is 17% at the C_{s_index} of 0.0121\$. Cost can also be extracted from the graph of C_{s_index}; approx. a 92.5% satisfaction level can be achieved by spending 4.9\$ per day, as shown in Figure 10. A set of Pareto-fronts obtained by simulating load demand without RER and ESS using MGWASA are saved in the archive. In the next section, these solutions are compared with the case where RER and ESS are integrated with the system.

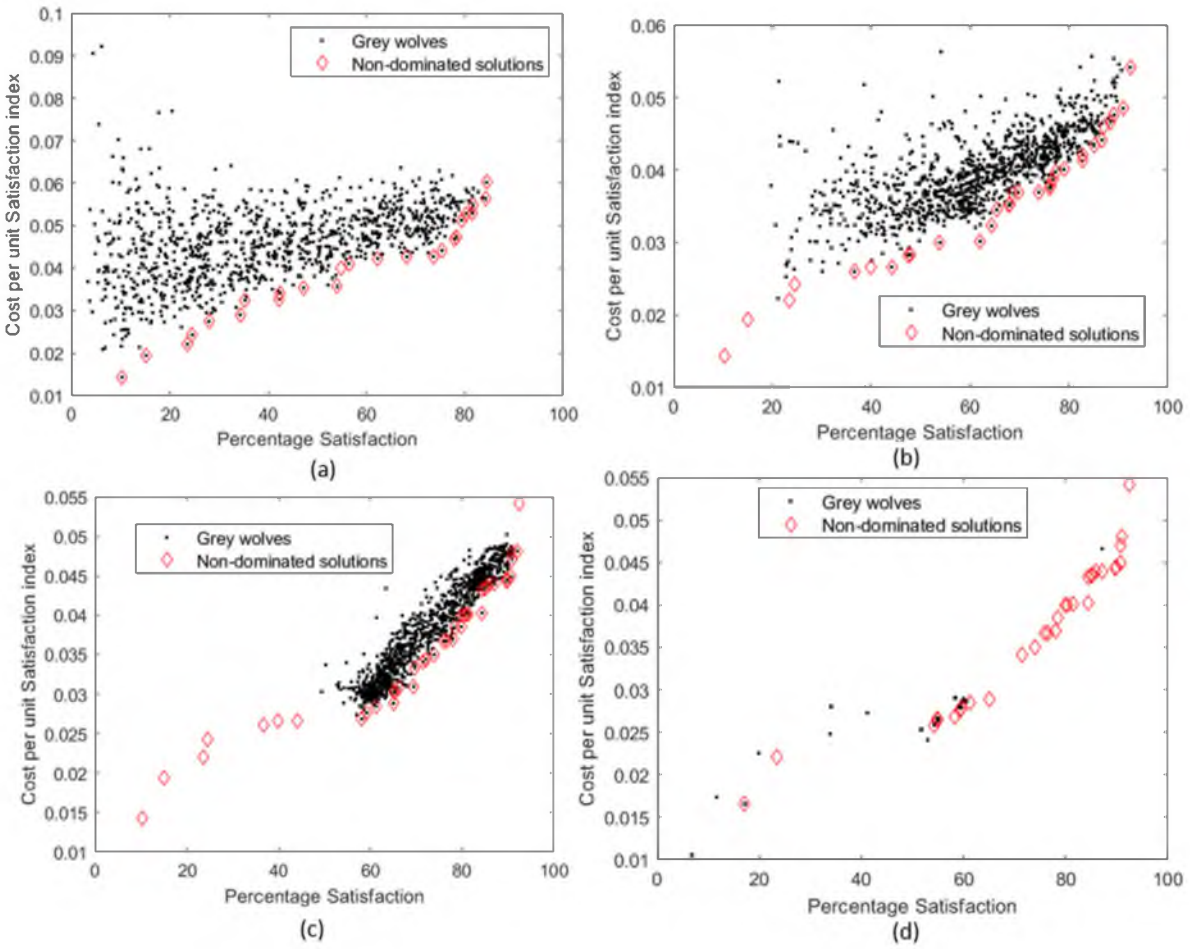

Figure 9. Four iterations of MGWASA with non-dominated solutions and grey wolf populations. (**a**) first iteration of MGWASA 1000 initial population evolve according to objective functions cost per unit satisfaction and percentage satisfaction between 0 to 100 and 0.01 to 0.1. (**b**) 2nd iteration C_{sindex} reduced from 0.1 to 0.06 with the same satisfaction level from to 0 to 100. (**c**) in third iteration C_{sindex} further reduced to 0.055. (**d**) where as in d non dominated solutions are remain with optimal C_{sindex}.

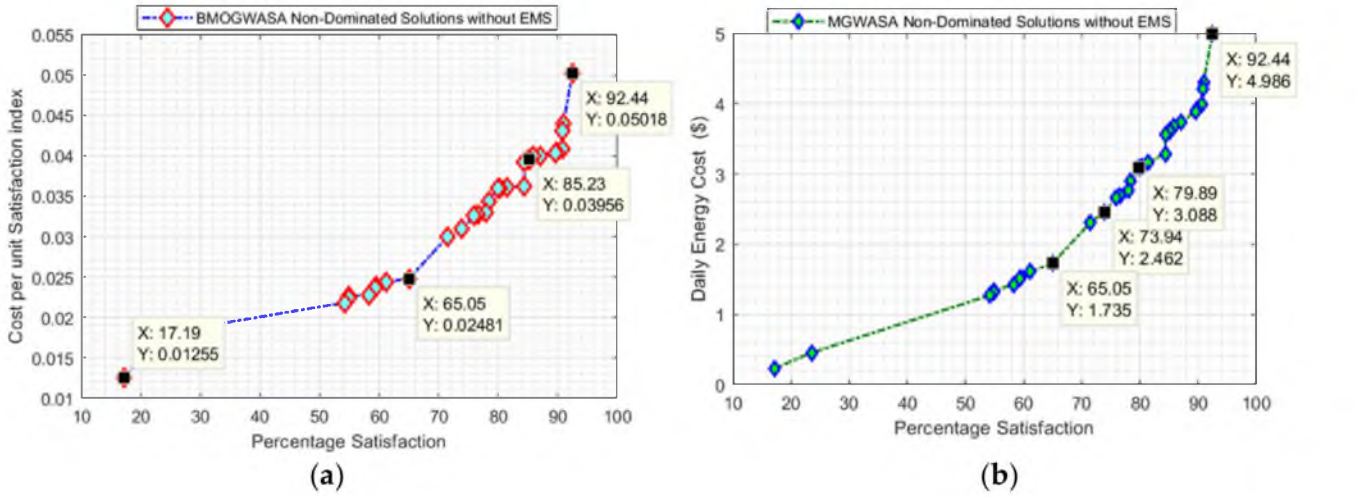

Figure 10. Relationship between (**a**) cost per unit satisfaction index and percentage satisfaction, and (**b**) daily energy cost and percentage satisfaction.

In Figure 11, fifty Pareto-front solutions saved in the archive, and the desired satisfaction levels are presented with different colours. A few solutions are selected and shown on the right for a better understanding. The trend indicates that the satisfaction level decreases with the decreasing cost. It can be seen that the percentage satisfaction value of 92.42% at C_{s_index} of ca. 0.05$ is the highest satisfaction value achieved during the optimization process. A median solution of 54% satisfaction with the C_{s_index} of 0.02$ provides a reasonable solution for consumers with a limited budget who cannot afford more costly scheduling patterns.

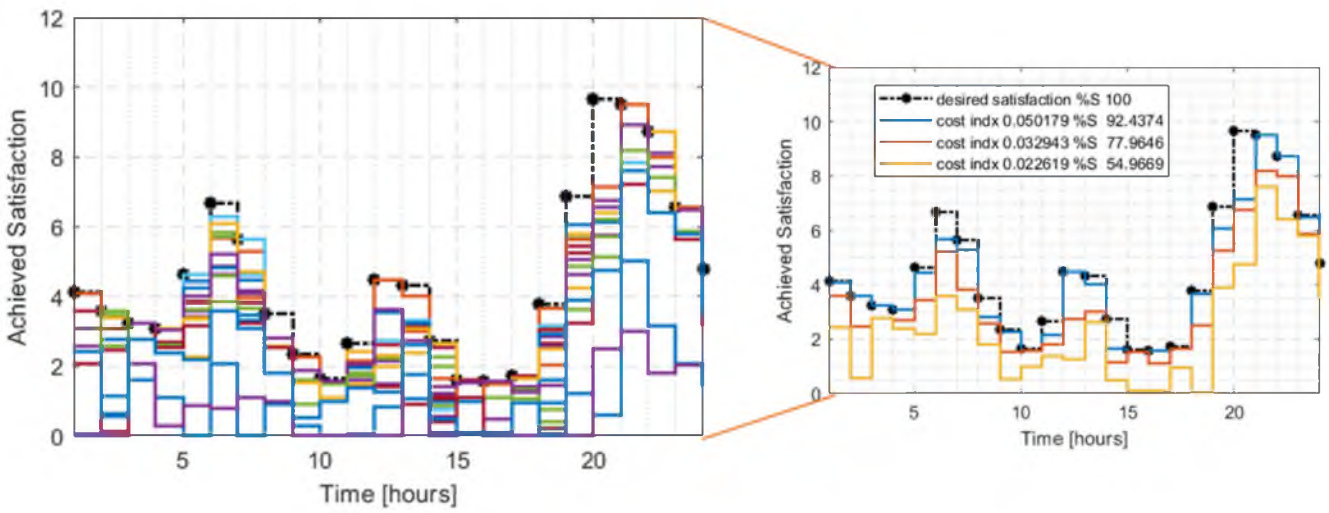

Figure 11. Obtained 50 Non-dominated solutions for summer without EMS.

7.2.2. Case 2: Appliance Scheduling Using MGWASA with Integration of EMS

In this case, the intelligent energy management scheme runs the load, including PV, ESS, and the utility grid.

The results of four iterations of MGWASA are shown in Figure 12, where it can be observed that the grey wolf population follows the best trade-off solutions between the cost per unit satisfaction index and percentage satisfaction. Integrating EMS in the optimization improves the satisfaction range from 13–90% to 86–96%, and the C_{s_index} range is reduced from 0.01–0.07 to 0.036–0.042, respectively. In the previous case, where EMS was not involved in the optimization process, 92.02% satisfaction was achieved against C_{s_index} of 0.05$ with daily energy cost of 4.9$, whereas in the second case, 95.55% of %*S* is achieved

against C_{s_index} of 0.041$ with a daily energy cost of 4.2$. Thus, showing an improvement of ca. 4% in %S while decreasing daily energy cost by ca. 17%.

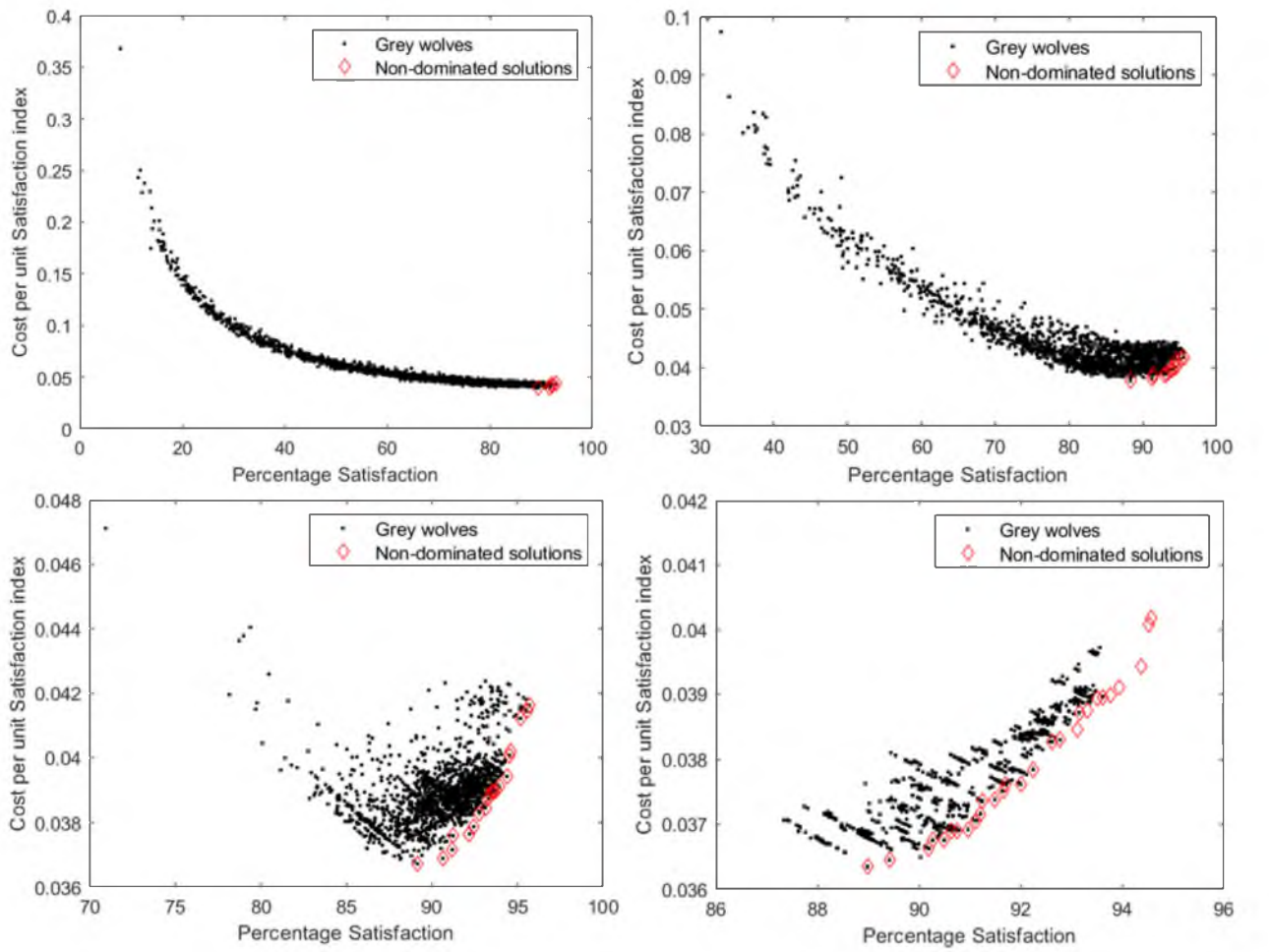

Figure 12. Four iterations of MGWASA with non-dominated solutions and grey wolf populations with the integration of RER-ESS.

In this case, MGWASA Pareto-front consists of 36 solutions, as shown in Figure 13. Four random solutions are selected in this figure to compare the performance with the previous case. It can be observed that the highest percentage satisfaction value of 95.5% is achieved at the C_{s_index} of 0.04$, implying that the satisfaction level is improved and the cost is decreased.

Figure 14 shows the Pareto optimal solutions saved in the archive after five iterations. In this case, 36 solutions are obtained at the end of the optimization. The satisfaction pattern for the whole day is also shown, and three solutions are compared with the desired value of consumer satisfaction. Minimum satisfaction of 88% is achieved at C_{s_index} of 0.03$, whereas a satisfaction level of 71% was previously achieved at a much higher C_{s_index} of 0.05$. This shows a cost difference of almost 0.03$ per unit satisfaction; in simplified terms, a daily cost reduction of 3$ is achieved in the second case.

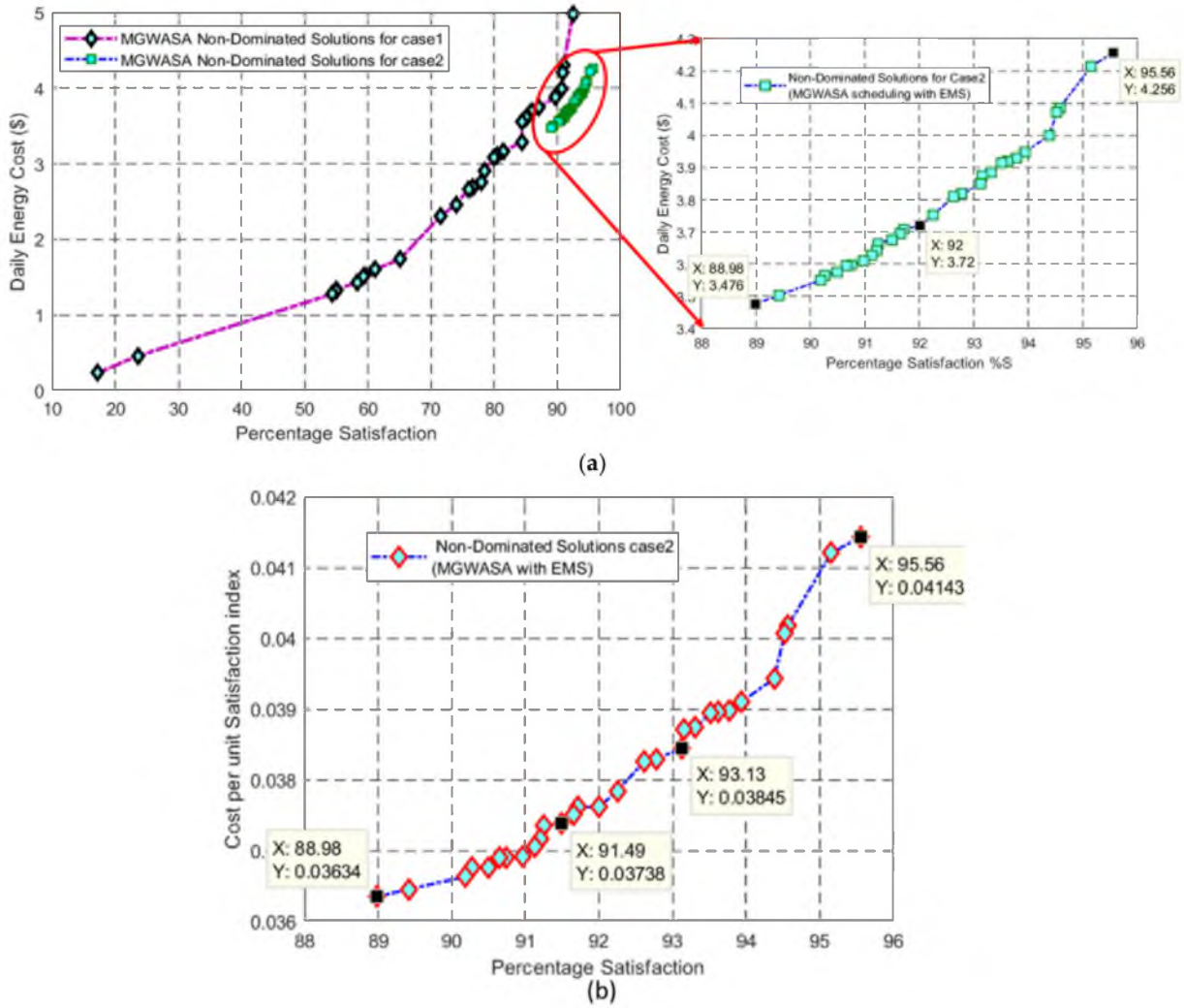

Figure 13. Relationship between (**a**) cost per unit satisfaction index and percentage satisfaction, and (**b**) cost and percentage satisfaction with integrating RER-ESS.

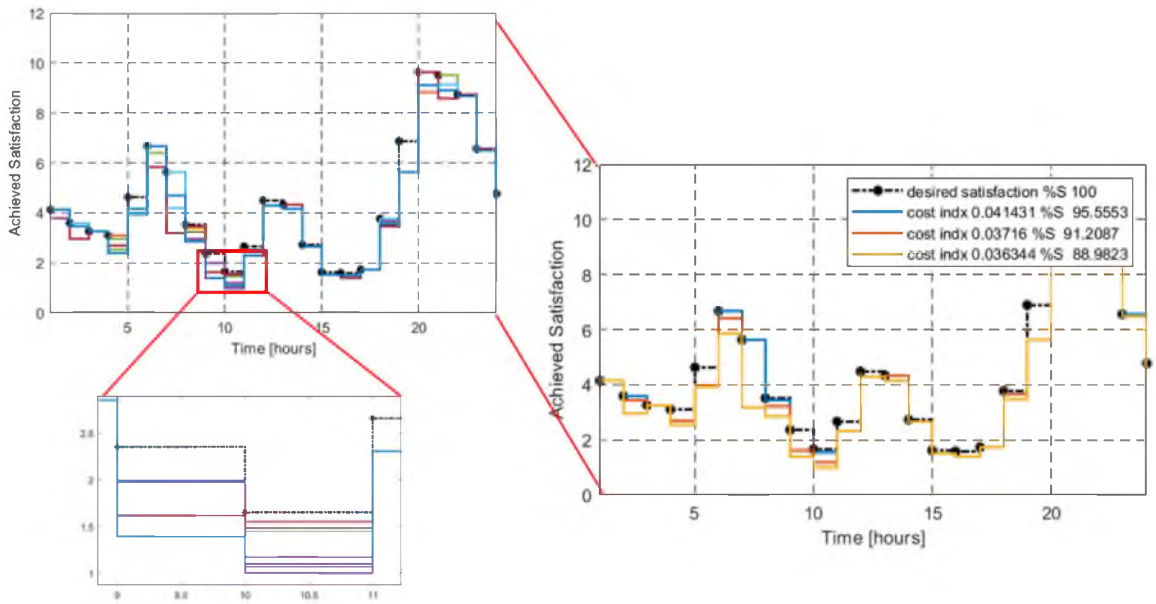

Figure 14. Obtained 36 Non-dominated solutions for a single day of summer while utilizing EMS.

7.2.3. Case 3: Ideal Load without Integration of EMS

The ideal load is extracted from the consumer satisfaction table. If the value of the satisfaction level is greater than zero, the device at that particular time slot will be considered in the ON state and vice versa. In Case 3, the ideal load is powered by the utility grid. Since the utility grid exclusively powers the user-preferred load demand without any optimization, 100% satisfaction is achieved at a staggering daily energy cost of 9.05$ with C_{s_index} of 0.082$.

7.2.4. Case 4: Ideal Load with Integration of EMS

In this case, the ideal load is powered by a mixture of the utility grid, PV, and ESS using the proposed EMS. The resultant energy mix for an entire day is shown in Figure 15.

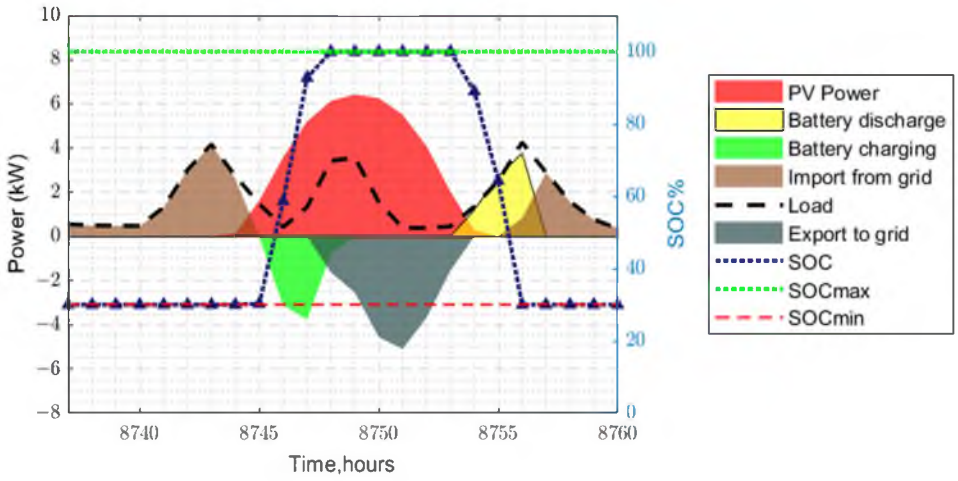

Figure 15. EMS energy mix analysis against the daily load extracted from the desired satisfaction table.

The energy transitions between the sources are according to the rules defined in the EMS and can be explained similarly to Figure 7. This case is simulated for the same day for which Case 1 and Case 2 were studied in detail. In this case, %S is 100% for the daily energy cost of 6.09$ with C_{s_index} 0.06$. A decrease in daily energy cost from 9.05$ to 6.09$ indicates the significance of optimal scheduling and EMS integration.

7.2.5. Case 5: Base Load without Integration of EMS

Base load is also a random load, in which any device can be switched on or off at any time without considering consumer preference. In Case 5, only the utility grid is considered for catering to the base load demand, which resulted in a poor %S of 38% with a substantially high daily energy cost of 8.09$.

7.2.6. Case 6: Base Load with Integration of EMS

In Case 6, the base load, discussed in the previous section, is run by a combination of the utility grid and EMS, utilizing RERs and ESS. In this case, a %S of 42% is achieved at a daily energy cost of 4$. Although there is a trivial increase of 4% in %S compared to Case 5, the daily energy cost has decreased considerably, again showcasing the significance of EMS in decreasing the cost. Nonetheless, there is still a need for proper load scheduling with the help of optimization.

7.2.7. Comparative Analysis of All the Cases

Figure 16 shows the seasonal variation in the daily cost and %S achieved for all six cases discussed in previous sections.

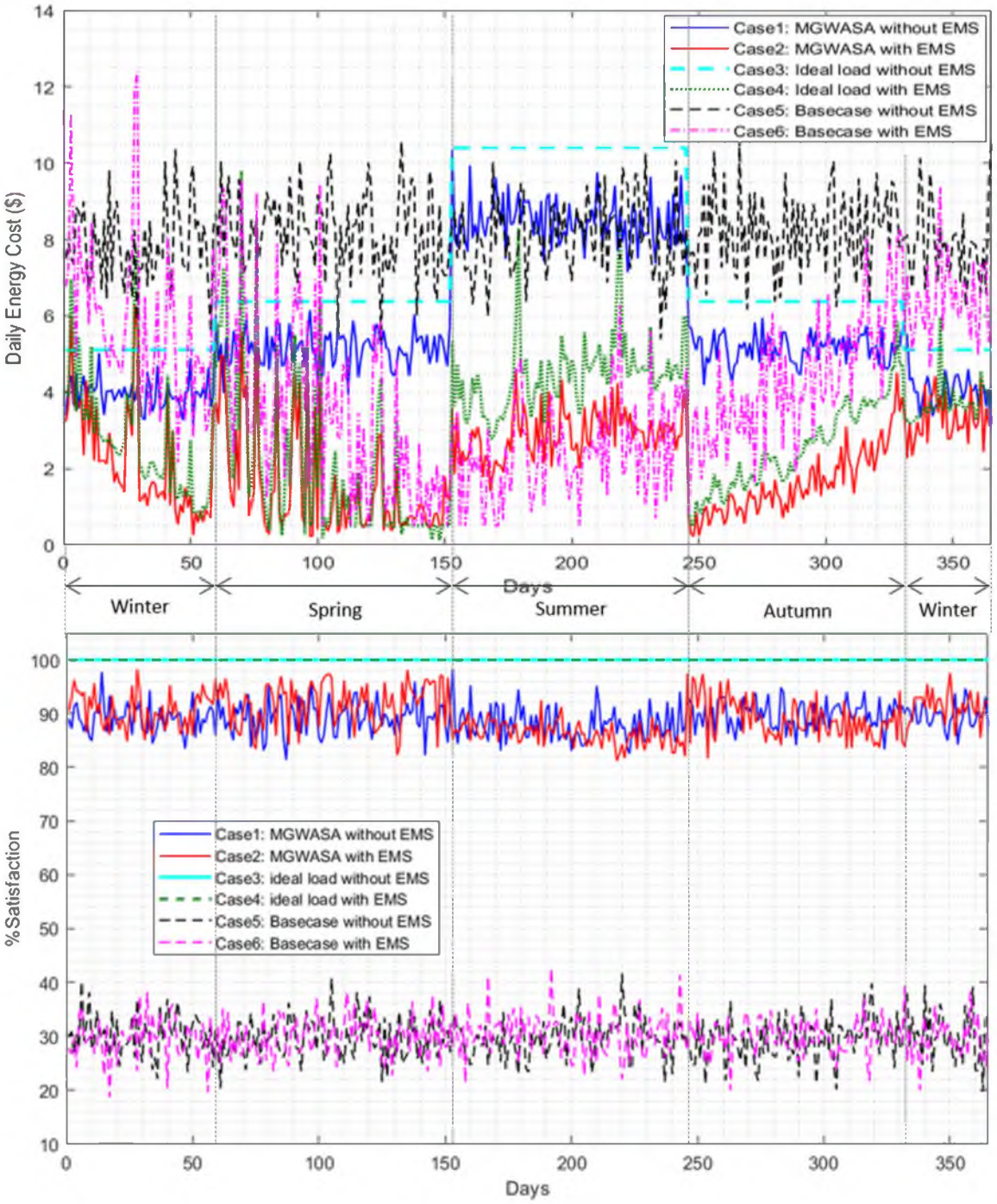

Figure 16. Annual comparative analysis of %satisfaction and daily energy cost for all the cases.

The summer season has a relatively higher daily cost, mainly due to air conditioning. In principle, the daily energy cost is considerably higher when the utility grid solely runs the load. Integration of EMS reduces the daily energy cost regardless of the load profile. Moreover, scheduling with MGWASA significantly improves the %S while reducing the average cost. Thus, MGWASA and EMS improve the system's performance in terms of daily energy cost and %S. Table 7 shows a comparative analysis of all the cases in daily energy cost and %S for a single day.

Table 7. Comparative analysis of all the cases with respect to daily energy cost and %S for a single day.

	Case 1	Case 2	Case 3	Case 4	Case 5	Case 6
	MGWASA		Ideal Load		Base Load	
	W/o EMS	With EMS	W/o EMS	With EMS	W/o EMS	With EMS
Daily energy cost ($)	4.99	4.25	9.05	6.02	8.09	4
%S	92.44	95.54	100	100	38	42

7.3. Comparative Analysis with the State-of-the-Art Algorithms

Figure 17 compares MGWASA with the other state-of-the-art multi-objective algorithms, NSGAII, MOBPSO, MOABC, and MOEA. The simulation showed that the proposed technique significantly improved consumer satisfaction with a minimum cost per unit satisfaction compared to other optimization algorithms. The highest achievable percentage satisfaction value using MGWASA, NSGAII, MOBPSO, MOABC, and MOEA is 97%, 95%, 90%, 92%, and 94%, respectively, against the optimum C_{s_index} of 0.049$, 0.052$, 0.048$, 0.0485$, and 0.05$, respectively. Hence, it can be concluded that in both objective functions, the highest optimum value is achieved by MGWASA. If the minimum satisfaction value is compared among all the algorithms, MGWASA provides 77% satisfaction, whereas NSGAII, MOBPSO, MOABC, and MOEA provide 66%, 63%, 72%, and 73% satisfaction, respectively. In terms of minimum C_{s_index}, MGWASA gives 0.335$, while 0.035$, 0.037$, 0.033$, and 0.0335$ are the minimum optimum C_{s_index} solutions obtained by NSGAII, MOBPSO, MOABC, and MOEA, respectively. Thus, the proposed advanced MGWASA outperformed all the other state-of-the-art algorithms.

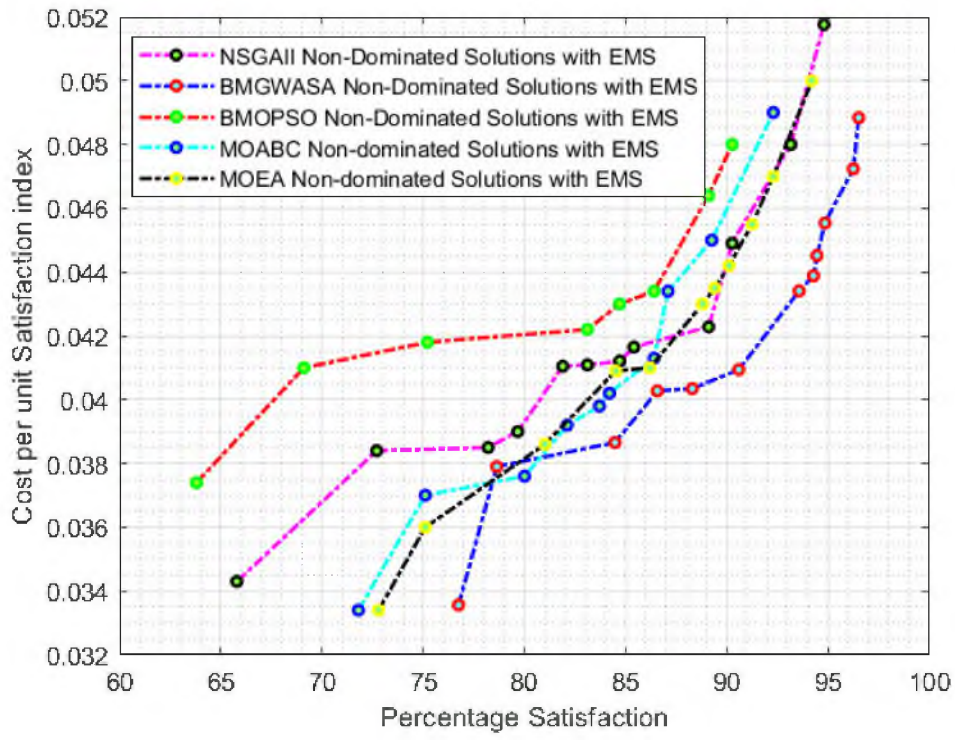

Figure 17. Comparative analysis of MGWASA, NSGAII, MOBPSO, MOABC, and MOEA.

To further investigate the performance of the proposed MGWASA, the output of the proposed algorithms is also compared for different cases (a) in the absence of RER, (b) in the presence of RER, and (c) when only the utility grid supplies the power to the un-optimized loads. With efficient utilization of EMS by MGWASA, approximately 93% satisfaction is achieved at the C_{s_index} of 0.049$. Whereas, when the loads are powered solely by the utility grid, the consumer satisfaction level decreases to 82% for nearly the same C_{s_index} value.

Moreover, in the Case 3, without optimization and EMS, 100% satisfaction is achieved but at a considerably higher C_{s_index} of 0.06$, as shown in Figure 18.

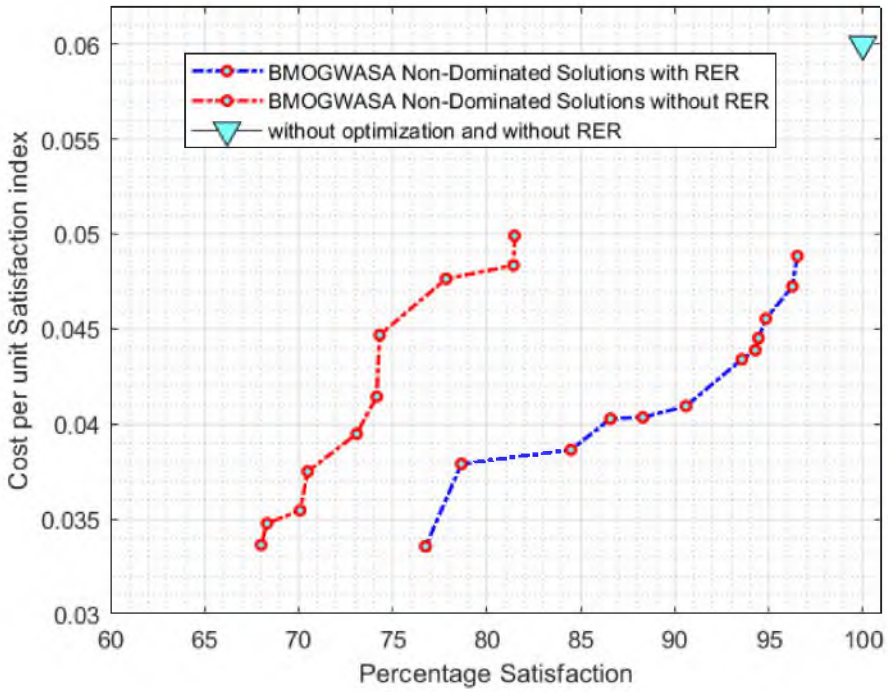

Figure 18. Comparison of MGWASA, percentage satisfaction, and cost per unit satisfaction index for three test cases.

7.4. Energy Flow and Balance Analysis

The impact of various seasons and scheduling cases on PV energy production and surplus energy is shown in Figure 19. The surplus energy refers to the PV energy remaining after satisfying the load demand and battery charging at a time interval t, which is exported to the utility grid. It is evident from Figure 19 that the highest amount of PV energy is produced in the summer season due to the larger value of solar irradiance and longer durations of daily sunshine. On the other hand, the winter season has shorter days and smaller irradiance values, resulting in a relatively low amount of PV energy production. To be exact, 37% less PV energy is produced in winter compared to summer. It can also be observed that the surplus PV energy (grid export) corresponds to the amount of PV energy production in the respective season. However, in the optimal case, overall surplus PV energy is comparatively low due to an efficient load scheduling by the proposed algorithm. Furthermore, the results indicate that although summer has more PV energy production than the spring season, the amount of respective surplus energy is not in accordance with the production. This is attributed to the high energy demand during the summer season. Such analysis can also be performed for the project's lifetime by adjusting the model's input parameters.

A study was also conducted on the system's annual PV energy utilization. Figure 20 shows how the PV energy contributes in different ways, for three cases, inside the system. In principle, there are four possible ways the PV energy is utilized: (1) PV energy is directly consumed by the load, (2) surplus PV energy is used to charge the batteries, (3) the remaining PV energy from (1) and (2) is exported to the utility grid provided that PEL is not reached, and (4) any surplus energy above PEL is dumped. The most cost-effective utilization of PV energy is its direct use for powering residential loads. Therefore, an efficient scheduling algorithm aims to schedule the maximum residential load during the PV production hours. It can be seen in Figure 20 that 41% of the produced PV energy is utilized for directly powering the loads in the optimal case. On the other hand, other cases do not take maximum advantage of the PV energy and only use 26% to 30% of the produced

PV energy. However, there is no significant difference regarding the PV energy contribution in charging the batteries. The part of the PV energy unused by the loads and batteries is exported to the utility grid. This is a less preferred way of PV energy usage because the export tariff of the utility grid is generally cheaper. The optimal case substantially reduces the energy export to the utility grid compared to other cases, ensuring the effective utilization of PV energy. In base and ideal cases, more than 50% of the produced PV energy is exported to the utility grid on a cheaper tariff, which is inefficient utilization of the RERs. Moreover, in the base case, 1% of the PV energy is dumped, the least preferred utilization of the PV energy.

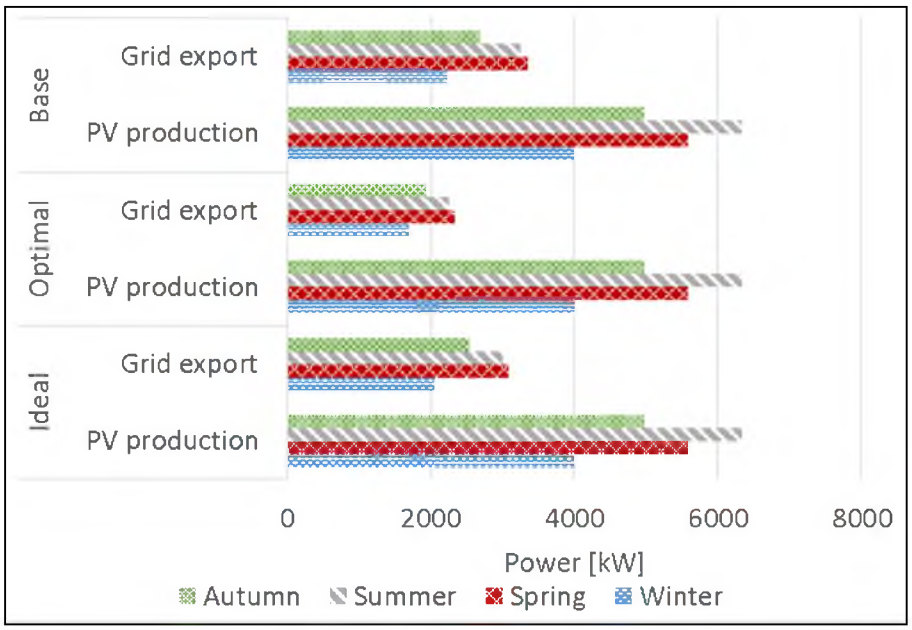

Figure 19. Seasonal PV energy production and impact of scheduling cases on the export of surplus PV energy to the utility grid.

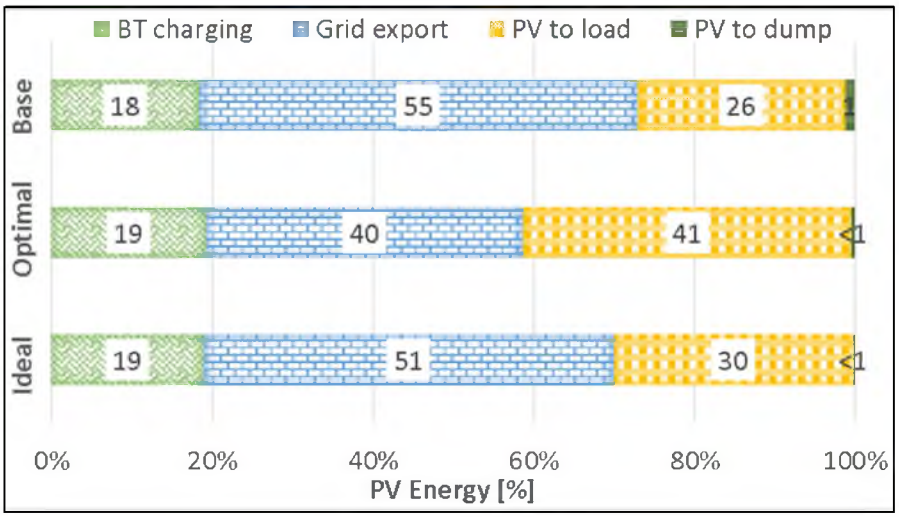

Figure 20. Analysis of PV energy utilization for different cases.

An analytical comparison of annual energy exported to and imported from the utility grid was also carried out for three different scheduling cases, as depicted in Figure 21. The results indicate that a relatively higher amount of energy is exported and imported in the base case, followed by ideal and optimal cases. In the optimal case, the system dependency on costly utility grid energy is minimum. Both base and ideal cases, though, export a

comparatively larger amount of energy to the utility grid; it is tariffed at a much lower price, making it less cost-effective. It can also be noted that the base case exhibits the worst energy import-export balance.

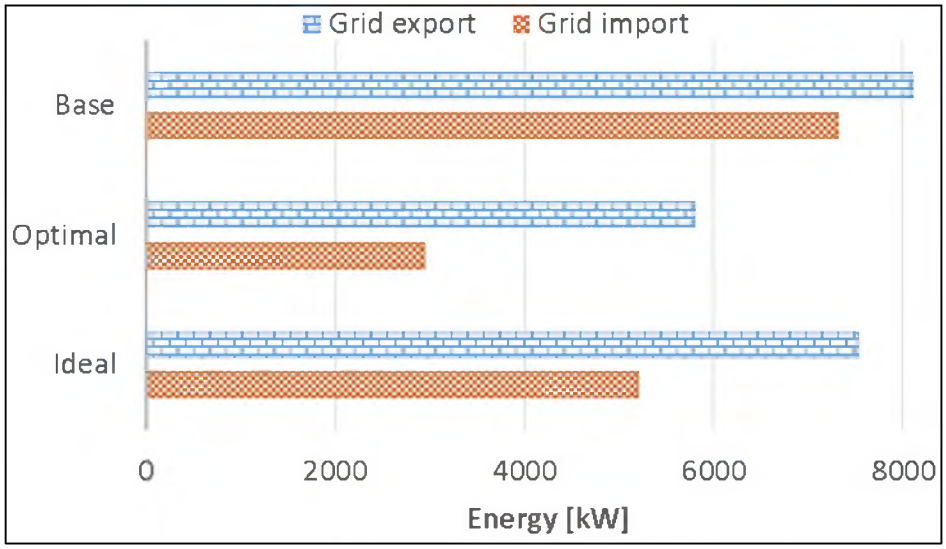

Figure 21. Comparative analysis of energy export/import to/from the utility grid for three different cases.

An efficient scheduling algorithm aims to cater majority of its residential load using domestic resources while reducing the energy import from the utility grid. Figure 22 shows the percentage contributions of different energy sources to meet the annual energy demand for three cases. The analysis shown in Figure 22 highlights the efficacy of the proposed scheduling algorithm. It can be noticed that approximately 69% of residential load demand is catered by PV energy and the batteries for optimally scheduled loads. On the other hand, ideal and base cases rely significantly on the utility grid and fulfill only 59% and 52% of their energy requirements from domestic resources.

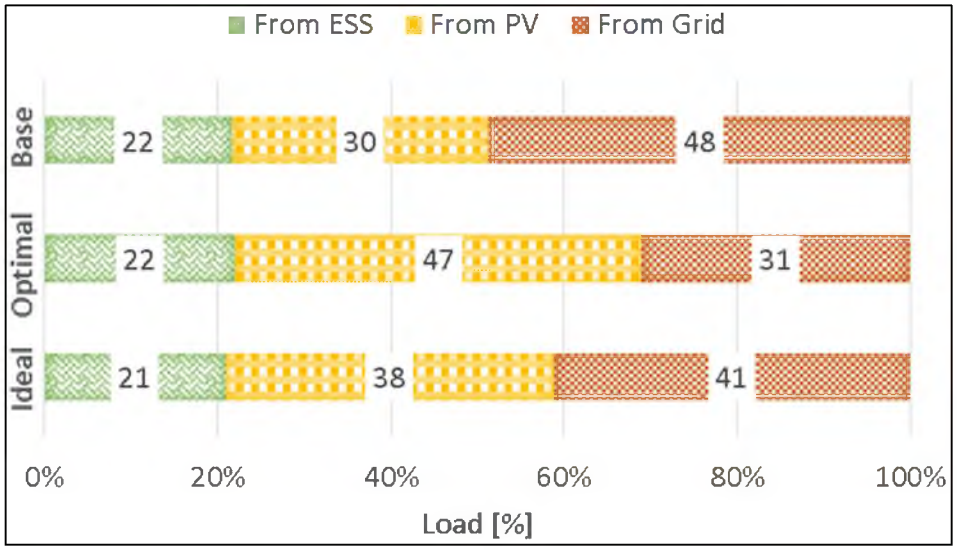

Figure 22. Analysis of different energy contributions in fulfillment of annual energy demand for three scheduling cases.

Based on Figures 20–22, a comprehensive energy balance analysis for the proposed system with optimal scheduling is illustrated in Figure 23.

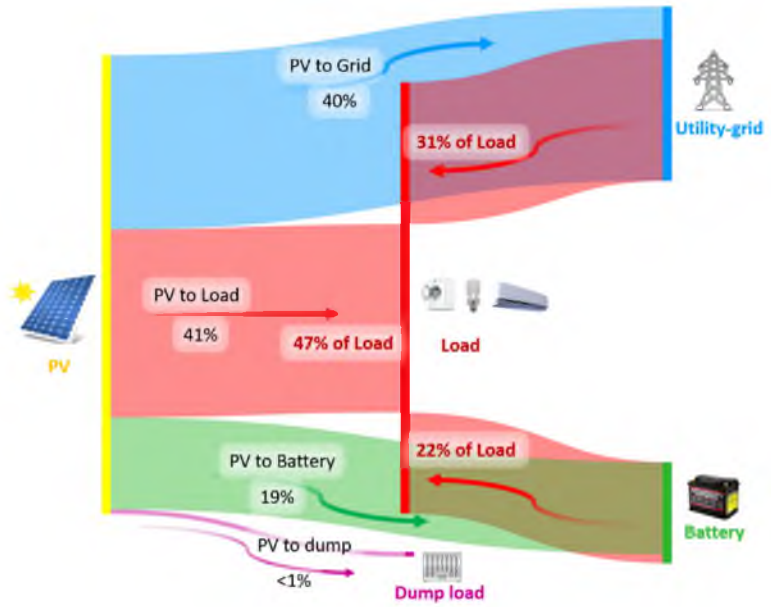

Figure 23. Energy flow analysis in the proposed system with optimal scheduling.

7.5. Sensitivity Analysis

7.5.1. Impact of PV Energy Production Capacity

PV energy serves as the alternative energy source for the smart home, which makes its production capacity a vital parameter. This section analyzes the impact of PV capacity variation on the overall system. Such analysis enables the designer to select the appropriate PV capacity in accordance with individual requirements. The sensitivity analysis was performed by varying the number of PV panels from 2 to 70. The optimal scheduling values with maximum satisfaction level obtained in Case 2 MGWASA for the whole year are considered. Each PV panel has a power rating of 275 W (Table 2). The obtained sensitivity curves are shown in Figure 24. It can be seen that the increase in the number of PV panels, to a certain level, leads to a reduction in annual energy cost because the load demand is increasingly met by cheaper PV energy instead of the costly utility grid, and the surplus PV energy is either used to charge the batteries or exported to the grid. However, after a certain limit, a further increase in the PV panel count is counterproductive because the surplus PV energy is more than the PEL of the utility grid and an increasing amount of PV energy has to be dumped. The optimal number of PV panels obtained using GA (Section 7.1) against the respective annual energy cost and the amount of export/dump energies are indicated in Figure 24.

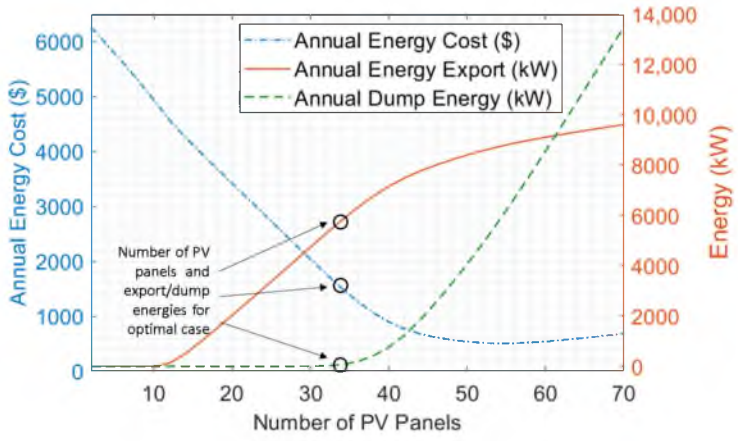

Figure 24. Sensitivity analysis: impact of PV production capacity on the annual energy cost, export, and dump energies for maximum satisfaction value from Case 2 MGWASA.

7.5.2. Impact of Battery Capacity

This section investigates the effect of battery capacity variation in smart homes. For this analysis, the maximum satisfaction level obtained in Case 2 MGWASA for the entire year is considered. The sensitivity adjustment of the battery capacity was made from 2 kW to 40 kW. The sensitivity curve obtained is shown in Figure 25. The right and left ordinates depict the annual energy cost ($), annual energy imported from the utility grid (kW), and annual battery charging (kW). It can be observed from Figure 25 that an increase in the battery capacity also increases the annual cost very rapidly. The annual battery charging also follows this trend. However, after a certain point (around 22 kW battery capacity), the pace of increment slows down. This happens due to the fact that the amount of PV energy production is fixed and approaching the limit of charging the battery even when the battery capacity is increasing. Similarly, energy import reduces with increasing battery capacity and reaches a trivial value near 40 kW battery capacity. This happens because an increasing amount of PV energy is available via battery to cater to the load demand. The energy import curve also shows a reduction in the pace of decrement for battery capacity values above 22 kW. The optimal battery capacity obtained using GA (Section 7.1) and respective annual cost, energy import, and battery charging are marked in the figure for reference. This analysis aids the designer in the selection of optimal battery capacity based on individual preferences.

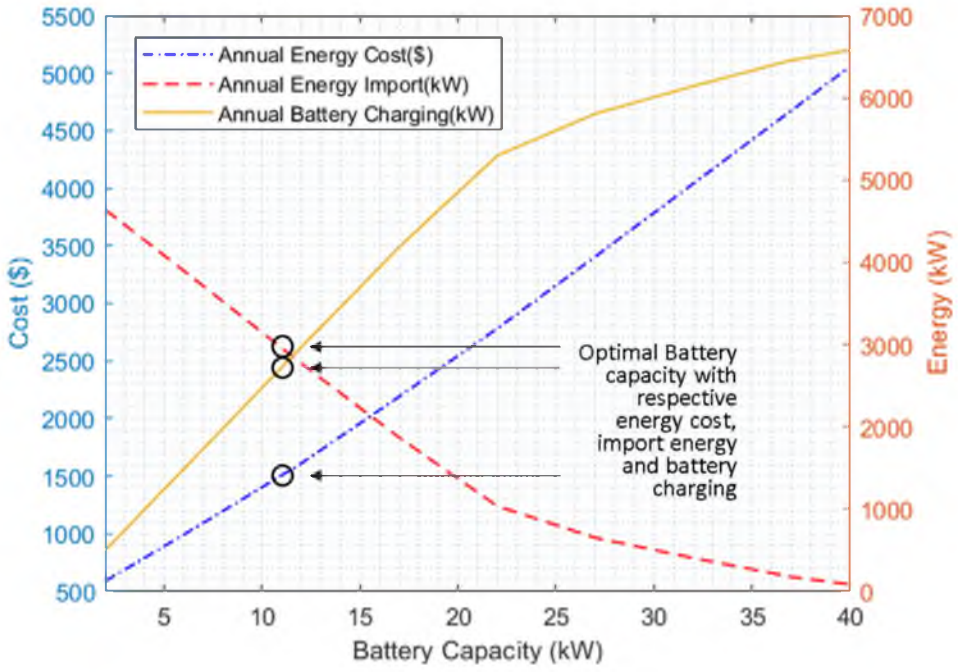

Figure 25. Sensitivity analysis: impact of battery capacity on the annual energy cost, battery charging, and energy import for maximum satisfaction value from Case 2 MGWASA.

7.5.3. Impact of Climatological Conditions, Battery Health, and Tariff Price

Apart from optimal scheduling, several other factors play a decisive role in determining the cost of energy. Climatological conditions such as irradiance, cloud cover, and precipitation directly dictate the amount of PV energy production. On the other hand, batteries are not only expensive, but they also have a shorter service time, which makes battery health a crucial parameter. Lastly, the tariff price of the utility grid has a direct impact on the cost of energy. In recent times, crude oil prices have gone down, which influences the tariff price because crude oil-based thermal power plants have the largest share in total power generation in Pakistan. In light of the above-mentioned facts, the effect of PV energy production, battery health, and tariff price on the annual energy cost was analyzed. To perform this sensitivity analysis, optimal size (Section 7.1) values were used.

Figure 26 shows the sensitivity graphs obtained via sensitivity adjustment performed using 20% decrements. The nominal values (without adjustment) of the sensitivity parameters are marked by the "Base" point on the sensitivity curve's abscissa. A significant increase in the annual energy cost can be observed for decreasing PV energy values because the dependency on the costly utility grid increases with lower PV energy production. The sensitivity curve of battery health against annual energy cost shows a similar trend. However, battery health has a relatively smaller impact on the annual energy cost compared to PV energy. This is attributed to the fact that the battery size is relatively small compared to the daily residential load. The tariff price, on the other hand, also has a significant impact on the value of annual energy costs. The annual energy cost rises in accordance with the price of the tariff.

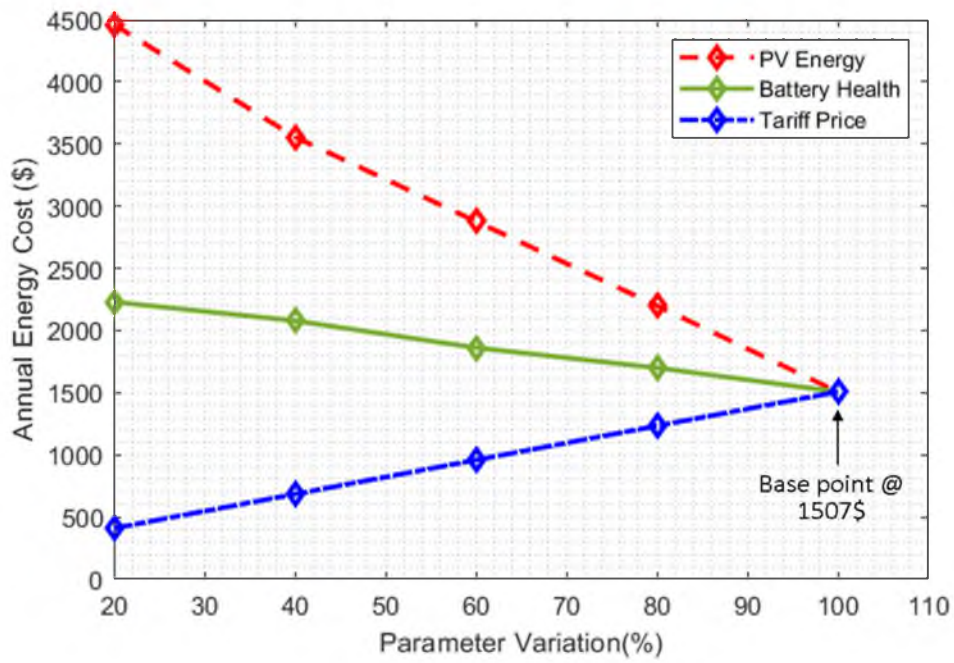

Figure 26. Sensitivity analysis: impact of PV energy, battery health, and tariff price on the annual energy cost for maximum satisfaction value from Case 2 MGWASA.

7.6. Analysis of Net Present Cost of the System

The total net present cost (NPC), and associated categories, of integral components of the proposed system are shown in Figure 27. It can be observed from Figure 27a that batteries have the overall highest total NPC of ca. 46%, followed by PV (31%) and inverter (23%). However, the breakdown of system cash flow categories (Figure 27b) highlights that the seemingly high cost of batteries is distributed over the project's entire lifetime owing to their shorter lifespan, requiring frequent replacement. On the contrary, the PV module's procurement cost has the biggest capital cost share. However, the impact on the overall system cost is comparatively smaller due to its longer lifespan. It can also be seen that the capital cost of the inverter is higher than batteries. However, they are only replaced once during the project lifetime, resulting in a smaller effect on total NPC. Unlike inverters, there is also O&M cost associated with PV modules and batteries. The total NPC was calculated to be ca. 21,700$ divided into capital cost, O&M cost, and replacement cost, having 46%, 4%, and 50% shares, respectively.

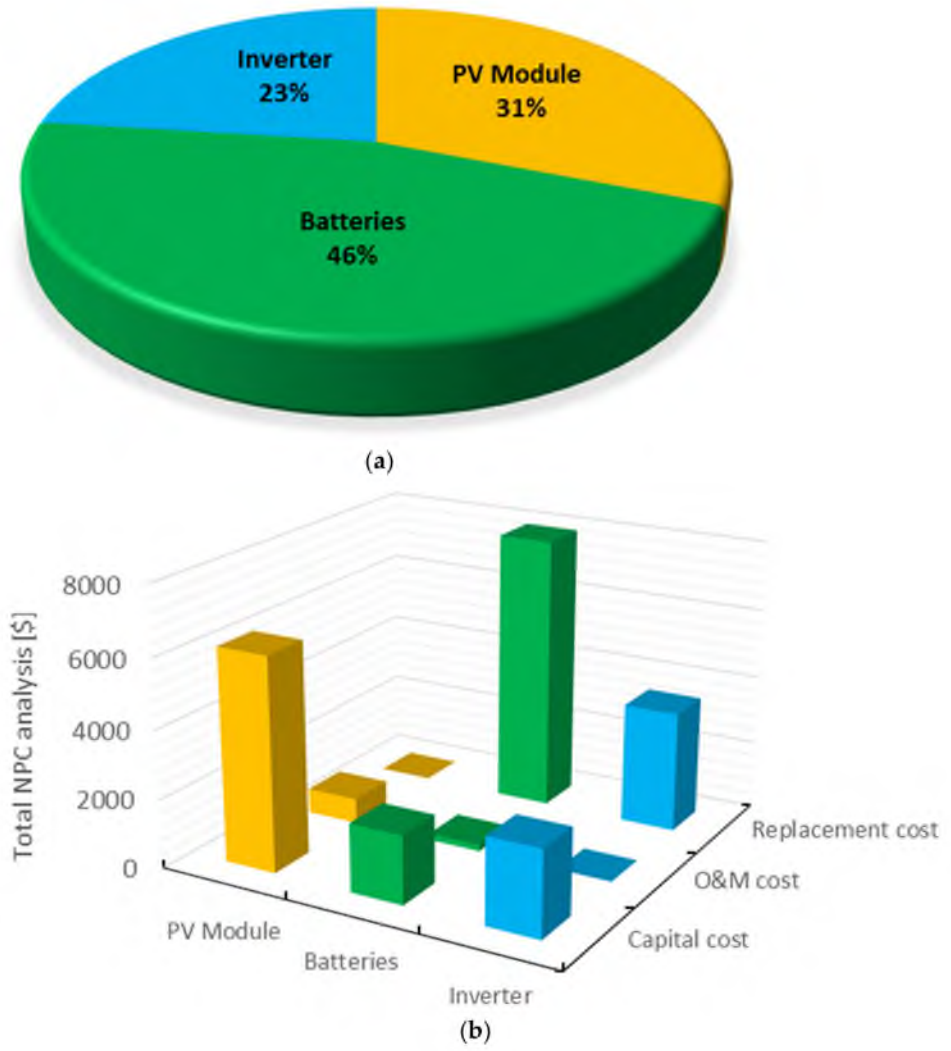

Figure 27. (**a**) Component and (**b**) cash flow category-wise breakdown of the total NPC of the proposed system.

7.7. Energy Cost Analysis and Cash Payback Period

In order to validate the profitability of the study, a comprehensive analysis of the energy cost, project expenses, and revenue is carried out to determine the cash payback period (CPP). Figure 28 shows the annual energy cost analysis of all three cases, both with and without the integration of RER and ESS. The base case's highest annual energy cost of 3221$ is obtained, excluding the proposed scheme and EMS. The least annual energy cost of 1507$ is obtained for the optimal case, where optimal load scheduling via MGWASA and EMS are considered. The annual energy cost of the ideal case resides relatively in between the base and optimal cases. It is evident from Figure 28 that the integration of RER and ESS, regardless of the case, has a substantial impact on the annual energy bill. From the annual energy cost analysis, it is calculated that a yearly profit gain (PG_i) of 1191$ is achievable.

The CPP of the investment in the PV module and ESS is calculated by evaluating the net present value (NPV) of the system for each year of the project lifespan [41]:

$$NPV = -(C_{PV} + CC_{ESS} + CC_{Inv}) + \sum_{i=1}^{n} \frac{NCF_i}{(1+r)^i} \quad (36)$$

where C_{PV}, CC_{ESS}, and CC_{Inv} represent the cost incurred on the PV module, ESS, and inverter, respectively. While n denotes the project's lifespan, NCF shows net cash flow, and

r represents the incentive in the form of a discount by the government. The yearly NFC is calculated by:

$$NCF_i = PG_i - OM_i \tag{37}$$

where PG_i shows the profit gained for the year i compared to the ideal case (w/o EMS), while OM_i represents the annual O&M spending on the PV and ESS.

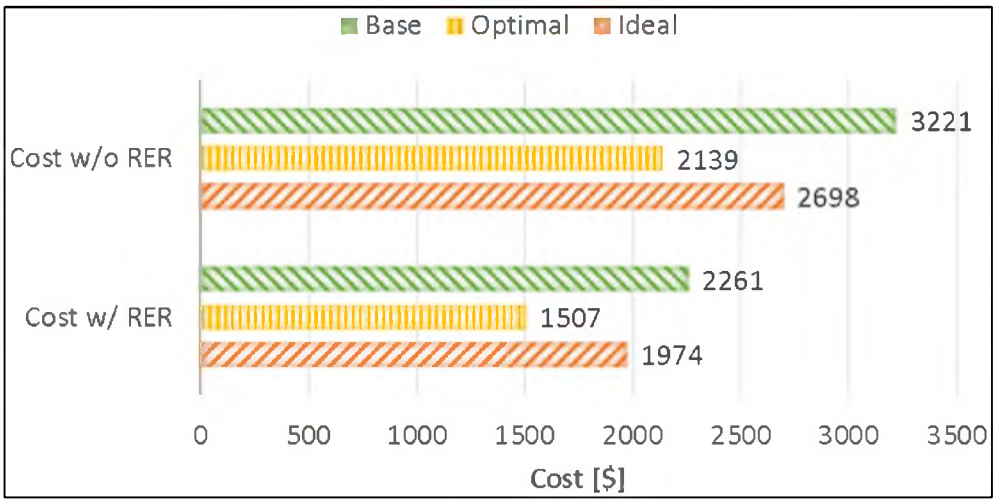

Figure 28. Annual energy cost analysis for all three cases with and without integration of RER and ESS.

Taking an inflation rate of 3%, the CPP is calculated to be ca. 12.5 years, as shown in Figure 29, for a properly implemented project. Furthermore, an estimated net profit of 8075$ is achievable after 25 years of service. Figure 29 indicates that the proposed system is economically beneficial and offers a low-risk investment opportunity owing to a short CPP. Such a system can contribute significantly towards sustainable global development goals by reducing greenhouse gas emissions and increasing power reliability.

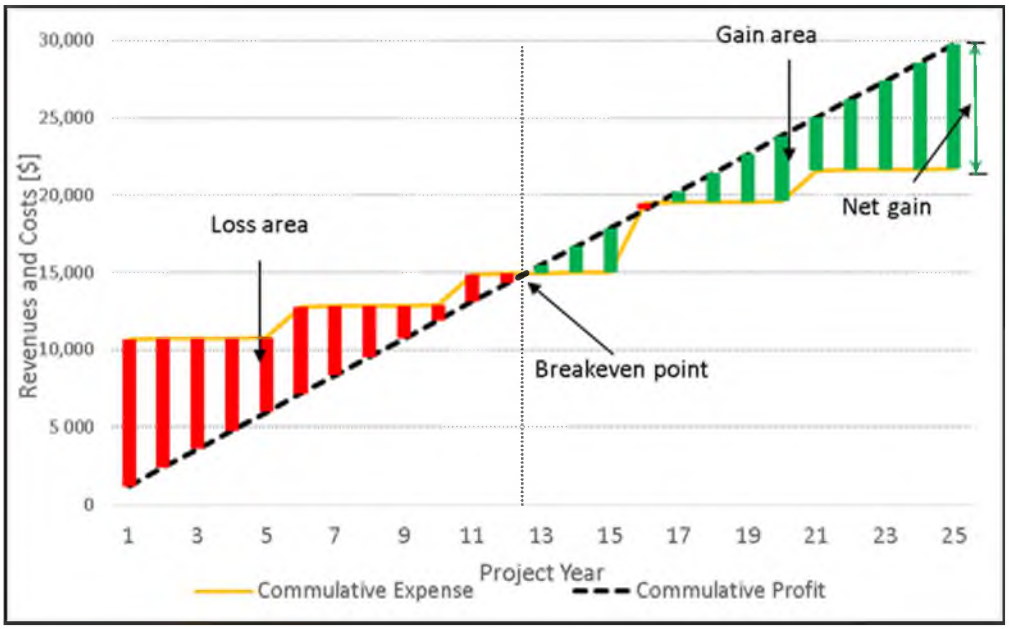

Figure 29. CPP analysis of the proposed system over the project lifetime.

8. Conclusions and Outlook

A consumer preference-based EMS utilizing MGWASA has been presented in this paper. The concept of absolute consumer satisfaction has been realized by assigning time-varying preferences to the appliances in the time and device-based domain. MGWASA was used to generate an optimal appliance scheduling pattern to maximize consumer satisfaction at a reduced cost. Furthermore, GA has been used to find the optimal capacity of the employed hybrid RER-ESS. The effectiveness of the proposed technique has been demonstrated by simulating a smart home with different cases and scheduling scenarios. The simulation results showed that the proposed technique significantly improved consumer satisfaction with a minimum cost per unit satisfaction compared to other scheduling scenarios and optimization algorithms like NSGAII, MOBPSO, MOABC, and MOEA. MGWASA yields better results as it offers the optimum C_{s_index} of \$0.049 with a %S of 97%, compared to NSGAII, MOBPSO, MOABC, and MOEA, which yield optimum solutions of 97%, 95%, 90%, 92%, and 94% percent satisfaction at a relatively expensive C_{s_index} of 0.052\$, 0.048\$, 0.0485\$, and 0.05\$, respectively. Further analysis of the simulation results has revealed that the proposed technique has achieved 44% annual energy cost reduction by optimally scheduling the residential loads so that the PV is 20% more efficiently utilized compared to the base scenario.

Since the scope of this work was limited to the TOU pricing scheme for the entire scheduling duration, it is recommended that future work focuses on the dynamic pricing scheme, which may also consider the time and duration of appliance operation. In addition, the current framework considered the smart home as a single entity; hence, a single consumer preference was considered. It is possible to extend the current work to a scenario where multiple consumers with conflicting preferences are living in a smart home.

Author Contributions: Conceptualization, S.A. and S.M.A. (Shahrin Md Ayob); methodology, A.L.B.; software, L.A. and Q.A.-T.; validation, S.A. and M.T.; formal analysis, S.A. and M.T.; investigation, S.M.A. (Shahrin Md Ayob) and C.W.T.; resources, S.A.; data curation, S.A.; writing—original draft preparation, S.A. and M.T.; writing—review and editing, S.A., M.T. and S.M.A. (Shahrin Md Ayob); visualization, R.A.; supervision, S.M.A. (Shahrin Md Ayob) and C.W.T.; project administration, S.M.A. (Saad M. Arif); funding acquisition, S.M.A. (Saad M. Arif). All authors have read and agreed to the published version of the manuscript.

Funding: This research received no external funding.

Conflicts of Interest: The authors declare no conflict of interest.

References

1. Pamulapati, T.; Mallipeddi, R.; Lee, M. Multi-objective home appliance scheduling with implicit and interactive user satisfaction modelling. *Appl. Energy* **2020**, *267*, 114690. [CrossRef]
2. International Energy Agency. *Energy Statistics*; International Energy Agency: Paris, France, 2019.
3. U.S. Energy Information Administration. *Average Price of Electricity to Ultimate Customers*; U.S. Energy Information Administration: Washington, DC, USA, 2019.
4. El-Baz, W.; Tzscheutschler, P. Short-term smart learning electrical load prediction algorithm for home energy management systems. *Appl. Energy* **2015**, *147*, 10–19. [CrossRef]
5. Ogunjuyigbe, A.; Ayodele, T.; Oladimeji, O. Management of loads in residential buildings installed with PV system under intermittent solar irradiation using mixed integer linear programming. *Energy Build.* **2016**, *130*, 253–271. [CrossRef]
6. De Giorgi, M.G.; Congedo, P.M.; Malvoni, M.; Tarantino, M. Short-term power forecasting by statistical methods for photovoltaic plants in south Italy. In Proceedings of the fourth IMEKO TC19 Symposium on Environmental Instrumentation and Measurements: Protection Environment, Climate Changes and Pollution Control, Lecce, Italy, 3–4 June 2013; pp. 171–175.
7. Shewale, A.; Mokhade, A.; Funde, N.; Bokde, N.D. An overview of demand response in smart grid and optimization techniques for efficient residential appliance scheduling problem. *Energies* **2020**, *13*, 4266. [CrossRef]
8. Shaikh, P.H.; Nor, N.B.M.; Nallagownden, P.; Elamvazuthi, I.; Ibrahim, T. A review on optimized control systems for building energy and comfort management of smart sustainable buildings. *Renew. Sustain. Energy Rev.* **2014**, *34*, 409–429. [CrossRef]
9. Kim, J.; Hong, T.; Jeong, J.; Koo, C.; Jeong, K. An optimization model for selecting the optimal green systems by considering the thermal comfort and energy consumption. *Appl. Energy* **2016**, *169*, 682–695. [CrossRef]

10. Yahia, Z.; Pradhan, A. Multi-objective optimization of household appliance scheduling problem considering consumer preference and peak load reduction. *Sustain. Cities Soc.* **2020**, *55*, 102058. [CrossRef]
11. Seifi, A.; Moradi, M.H.; Abedini, M.; Jahangiri, A. An optimal programming among renewable energy resources and storage devices for responsive load integration in residential applications using hybrid of grey wolf and shark smell algorithms. *J. Energy Storage* **2020**, *27*, 101126. [CrossRef]
12. Lu, F.; Jin, W.; Zhang, L.; Wang, B.; Lin, Z.; Liu, S.; Chu, Z.; Zhang, J.; Leng, Z.; Wang, W. Multi-objective optimization model of electricity consumption for customers considering equipment consumption correlation. *Energy Rep.* **2021**, *7*, 209–215. [CrossRef]
13. Shi, K.; Li, D.; Gong, T.; Dong, M.; Gong, F.; Sun, Y. Smart community energy cost optimization taking user comfort level and renewable energy consumption rate into consideration. *Processes* **2019**, *7*, 63. [CrossRef]
14. Bakht, M.P.; Salam, Z.; Bhatti, A.R.; Sheikh, U.U.; Khan, N.; Anjum, W. Techno-economic modelling of hybrid energy system to overcome the load shedding problem: A case study of Pakistan. *PLoS ONE* **2022**, *17*, e0266660. [CrossRef] [PubMed]
15. Bakht, M.P.; Salam, Z.; Bhatti, A.R.; Anjum, W.; Khalid, S.A.; Khan, N. Stateflow-Based Energy Management Strategy for Hybrid Energy System to Mitigate Load Shedding. *Appl. Sci.* **2021**, *11*, 4601. [CrossRef]
16. Ogunjuyigbe, A.; Ayodele, T.; Akinola, O. User satisfaction-induced demand side load management in residential buildings with user budget constraint. *Appl. Energy* **2017**, *187*, 352–366. [CrossRef]
17. Elavarasan, R.M.; Leoponraj, S.; Vishnupriyan, J.; Dheeraj, A.; Sundar, G.G. Multi-Criteria Decision Analysis for user satisfaction-induced demand-side load management for an institutional building. *Renew. Energy* **2021**, *170*, 1396–1426. [CrossRef]
18. Ayub, S.; Ayob, S.M.; Tan, C.W.; Ayub, L.; Bukar, A.L. Optimal residence energy management with time and device-based preferences using an enhanced binary grey wolf optimization algorithm. *Sustain. Energy Technol. Assess.* **2020**, *41*, 100798. [CrossRef]
19. Dinh, H.T.; Yun, J.; Kim, D.M.; Lee, K.-H.; Kim, D. A home energy management system with renewable energy and energy storage utilizing main grid and electricity selling. *IEEE Access* **2020**, *8*, 49436–49450. [CrossRef]
20. Merdanoğlu, H.; Yakıcı, E.; Doğan, O.T.; Duran, S.; Karatas, M. Finding optimal schedules in a home energy management system. *Electr. Power Syst. Res.* **2020**, *182*, 106229. [CrossRef]
21. Liu, Y.; Xiao, L.; Yao, G.; Bu, S. Pricing-based demand response for a smart home with various types of household appliances considering customer satisfaction. *IEEE Access* **2019**, *7*, 86463–86472. [CrossRef]
22. Das, N.R.; Rai, S.C.; Nayak, A. A Model for Optimizing Cost of Energy and Dissatisfaction for Household Consumers in Smart Home. In *Advances in Intelligent Computing and Communication*; Springer: Berlin/Heidelberg, Germany, 2020; pp. 523–531.
23. Murugaperumal, K.; Raj, P.A.D.V. Integrated energy management system employing pre-emptive priority based load scheduling (PEPLS) approach at residential premises. *Energy* **2019**, *186*, 115815. [CrossRef]
24. Jindal, A.; Singh, M.; Kumar, N. Consumption-aware data analytical demand response scheme for peak load reduction in smart grid. *IEEE Trans. Ind. Electron.* **2018**, *65*, 8993–9004. [CrossRef]
25. Yahia, Z.; Pradhan, A. Optimal load scheduling of household appliances considering consumer preferences: An experimental analysis. *Energy* **2018**, *163*, 15–26. [CrossRef]
26. Mbungu, N.T.; Bansal, R.C.; Naidoo, R.M. Smart energy coordination of autonomous residential home. *IET Smart Grid* **2019**, *2*, 336–346. [CrossRef]
27. Bukar, A.L.; Tan, C.W.; Yiew, L.K.; Ayop, R.; Tan, W.-S. A rule-based energy management scheme for long-term optimal capacity planning of grid-independent microgrid optimized by multi-objective grasshopper optimization algorithm. *Energy Convers. Manag.* **2020**, *221*, 113161. [CrossRef] [PubMed]
28. Maleki, A.; Pourfayaz, F. Optimal sizing of autonomous hybrid photovoltaic/wind/battery power system with LPSP technology by using evolutionary algorithms. *Sol. Energy* **2015**, *115*, 471–483. [CrossRef]
29. Lan, H.; Wen, S.; Hong, Y.-Y.; David, C.Y.; Zhang, L. Optimal sizing of hybrid PV/diesel/battery in ship power system. *Appl. Energy* **2015**, *158*, 26–34. [CrossRef]
30. Ogunjuyigbe, A.; Ayodele, T.; Akinola, O. Optimal allocation and sizing of PV/Wind/Split-diesel/Battery hybrid energy system for minimizing life cycle cost, carbon emission and dump energy of remote residential building. *Appl. Energy* **2016**, *171*, 153–171. [CrossRef]
31. Zhang, L.; Barakat, G.; Yassine, A. Design and optimal sizing of hybrid PV/wind/diesel system with battery storage by using DIRECT search algorithm. In Proceedings of the 2012 15th International Power Electronics and Motion Control Conference (EPE/PEMC), Novi Sad, Serbia, 4–6 September 2012; pp. DS3b. 19-11–DS13b. 19-17.
32. Ayodele, T.; Ogunjuyigbe, A. Increasing household solar energy penetration through load partitioning based on quality of life: The case study of Nigeria. *Sustain. Cities Soc.* **2015**, *18*, 21–31. [CrossRef]
33. Yahiaoui, A.; Fodhil, F.; Benmansour, K.; Tadjine, M.; Cheggaga, N. Grey wolf optimizer for optimal design of hybrid renewable energy system PV-Diesel Generator-Battery: Application to the case of Djanet city of Algeria. *Sol. Energy* **2017**, *158*, 941–951. [CrossRef]
34. Setlhaolo, D.; Xia, X. Optimal scheduling of household appliances with a battery storage system and coordination. *Energy Build.* **2015**, *94*, 61–70. [CrossRef]
35. Khan, A.; Javaid, N.; Iqbal, M.N.; Anwar, N.; Ahmad, F. Time and device based priority induced demand side load management in smart home with consumer budget limit. In Proceedings of the 2018 IEEE 32nd international conference on Advanced Information Networking and Applications (AINA), Krakow, Poland, 16–18 May 2018; pp. 874–881.

36. Affolter, R. Pakistan—Solar Radiation Measurement Data. Available online: https://energydata.info/ (accessed on 14 March 2022).
37. Mirjalili, S.; Saremi, S.; Mirjalili, S.M.; dos Coelhod, L.S. Multi-objective grey wolf optimizer: A novel algorithm for multi-criterion optimization. *Expert Syst. Appl.* **2016**, *47*, 106–119. [CrossRef]
38. Al-Tashi, Q.; Kadir, S.J.A.; Rais, H.M.; Mirjalili, S.; Alhussian, H. Binary optimization using hybrid grey wolf optimization for feature selection. *IEEE Access* **2019**, *7*, 39496–39508. [CrossRef]
39. Emary, E.; Zawbaa, H.M.; Hassanien, A.E. Binary grey wolf optimization approaches for feature selection. *Neurocomputing* **2016**, *172*, 371–381. [CrossRef]
40. Arun, S.; Selvan, M. Intelligent residential energy management system for dynamic demand response in smart buildings. *IEEE Syst. J.* **2017**, *12*, 1329–1340. [CrossRef]
41. Singaravel, M.R.; Daniel, S.A. Sizing of hybrid PMSG-PV system for battery charging of electric vehicles. *Front. Energy* **2015**, *9*, 68–74. [CrossRef]